Energy 303 (2024) 131882

Contents lists available at ScienceDirect

Energy

journal homepage: www.elsevier.com/locate/energy

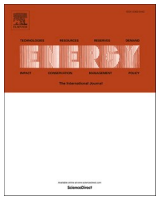

High-temperature heat pumps: Fundamentals, modelling approaches and applications

Hussam Jouhara [a,b,*], Alina Żabnieńska-Góra [c], Bertrand Delpech [a], Valentina Olabi [a], Tala El Samad [d], Abdulnaser Sayma [d]

[a] Heat Pipe and Thermal Management Research Group, College of Engineering, Design and Physical Sciences, Brunel University London, UB8 3PH, UK
[b] Vytautas Magnus University, Lithuania
[c] Faculty of Environmental Engineering, Wroclaw University of Science and Technology, Wybrzeze Wyspianskiego 27, 50-370, Wroclaw, Poland
[d] Department of Engineering, School of Science & Technology, City University of London, EC1V 0HB, UK

ARTICLE INFO

Handling editor: A. Olabi

Keywords:
High temperature heat pumps
Modelling
Refrigerants
Applications
Review

ABSTRACT

In March 2023, the European Parliament and Council reached a consensus to increase the binding renewable energy target (RES) to a minimum of 42.5 % by 2030, effectively doubling the proportion of RES from the 2020 baseline. This significant development aligns the EU more closely with the objectives of the European Green Deal and the REPowerEU initiative. High-temperature heat pumps (HTHP), due to their appropriateness for industrial-scale applications, integrate perfectly within this progressive trajectory. They enable waste heat generated by various production processes to be recovered (temperatures typically ranges from around 50 °C–100 °C) and subsequent use at temperatures above 100 °C, thus reducing the consumption of fossil fuels and greenhouse gas emissions. The high operating temperatures and pressures of HTHPs are challenging. They require an in-depth analysis of the system processes involved, taking into account refrigerants, efficient heat pump cycles and key components. One possibility for a preliminary analysis of vapour compression HTHP system performance without incurring the costs associated with manufacturing and testing the device is modelling. However, there is no comprehensive review of research work on possible software. Commonly, the researchers report on one chosen methodology and the tools used. This paper provides a comprehensive review of modelling approaches. It also discusses aspects related to the principles of operation, refrigerants and system components. Additionally, the paper presents an overview of vapour compression heat pump applications in various sectors. The literature review conducted indicates the need for further research and development of HTHP covering not only technological aspects but also software development.

1. Introduction

One of the policy objectives of the European Union, in alignment with the Paris Agreement, the Energy Union strategy (COM/2015/080), and broader climate policy, is the transition towards a low-carbon economy. Despite extensive efforts to curb global CO_2 emissions related to energy, these figures have continued to rise year on year, reaching 36.8 Gt in 2022 Fig. 1a [1]. Of this total, the industrial sector alone accounted for 9.0 Gt of CO_2 emissions [2]. Examining only energy-related greenhouse gas emissions, it is observed that CO_2 emissions from industrial processes and energy combustion constituted 89 % of the total. In 2022, compared to 2021, CO_2 emissions from industrial processes reduced by 102 Mt (1.7 %), driven by a 2 % reduction in steel production and a 10 % reduction in cement production in China Fig. 1b [1]. This reduction is attributed not only to the economic downturn, but also to the adoption of clean energy technologies, including heat pumps, among other factors. However, the report does not specify the share of individual systems or technologies.

In March 2023, the European Parliament and Council reached an agreement to elevate the binding renewable energy target to a minimum of 42.5 % by 2030, thereby doubling the share of RES compared to 2020. This significant step brings the EU closer to achieving the objectives outlined in the European Green Deal and the REPowerEU [3] initiative. According to data published by Eurostat in May 2023, the industrial

* Corresponding author. Heat Pipe and Thermal Management Research Group, College of Engineering, Design and Physical Sciences, Brunel University London, UB8 3PH, UK.
E-mail address: hussam.jouhara@brunel.ac.uk (H. Jouhara).

https://doi.org/10.1016/j.energy.2024.131882
Received 23 February 2024; Received in revised form 23 May 2024; Accepted 30 May 2024
Available online 31 May 2024

sector in the European Union was the third-largest final energy consumer in 2021, following transport and households, with a share of 25.6 % [4]. The energy products used in the industrial sector in 2021 are illustrated in Fig. 2a. A similar situation is observed in the UK, where an additional 4.2 % increase in energy consumption across most industrial sectors was recorded compared to 2020 [5]. Examining the variation in share of individual products for most industrial subsectors from 2021 to 2022, natural gas remains the primary source of energy, with the exception of the iron and steel industry where petroleum dominates, Fig. 2b. The proportion of renewable energy and biofuels in the European Union's industrial sector is steadily increasing year on year. Since 1990, it has nearly doubled, rising from 546 PJ to 976 PJ [4]. This energy is utilised not only for production processes, but also for heating, lighting, and air-conditioning.

The industrial sector presents itself as one of the most challenging sectors to decarbonise. This is primarily due to low-carbon technologies for many processes still being either under development or too expensive. In contrast, there exists a significant potential for energy recovery from distinct industrial processes, spanning a wide temperature range. This is discussed in greater detail in Section 6.

High-temperature heat pumps (HTHPs) facilitate recovery and subsequent utilisation of waste heat generated by various production processes, including drying, evaporation, food preparation, papermaking, and sterilization [6,7]. Their heat source temperatures range typically around 50 °C–100 °C and heat sink temperatures are above 100 °C. Therefore HTHP are a crucial component towards the path of decarbonisation due to their suitability for industrial-scale applications. They achieve this by diminishing the reliance on fossil fuels and reducing their consumption, thereby reducing greenhouse gas emissions.

As highlighted by Bianch et al. [8], both the Carnot efficiency and theoretical potential for waste heat recovery in European Union countries and industries are substantial. Notably, owing to the elevated temperatures of industrial waste heat sources, which may emerge from warm compressed air, wastewater, refrigeration fluid in chillers, or moist exhaust air, these represent crucial heat sources for heat pumps [6].

However, while conventional household heat pumps designed for heating or combined heating and cooling purposes are widely recognised and offered by numerous companies, High-Temperature Heat Pumps, devices capable of achieving heat sink temperatures above 100 °C, are not as well addressed in the existing literature. As observed by Adamson et al. [9], who analysed 49 distinct HP cycle configurations, 17 of which pertained to HTHPs, there exist substantial technological challenges, particularly pertaining to the compressor (such as compression stages exceeding 8 and the need for refrigerant compression to high pressures, exceeding 15 MPa for CO_2, along with the selection of a suitable refrigerant). This necessitates further in-depth analysis and research.

Industrial heat pumps are often developed for specific processes and temperature configurations, resulting in limitations for mass production, which increases design as well manufacturing costs. A number of research and review papers on high-temperature heat pumps have been published. These mainly focused on describing the types of HTHP cycles used or individual pump types and refrigerants. However, there has not

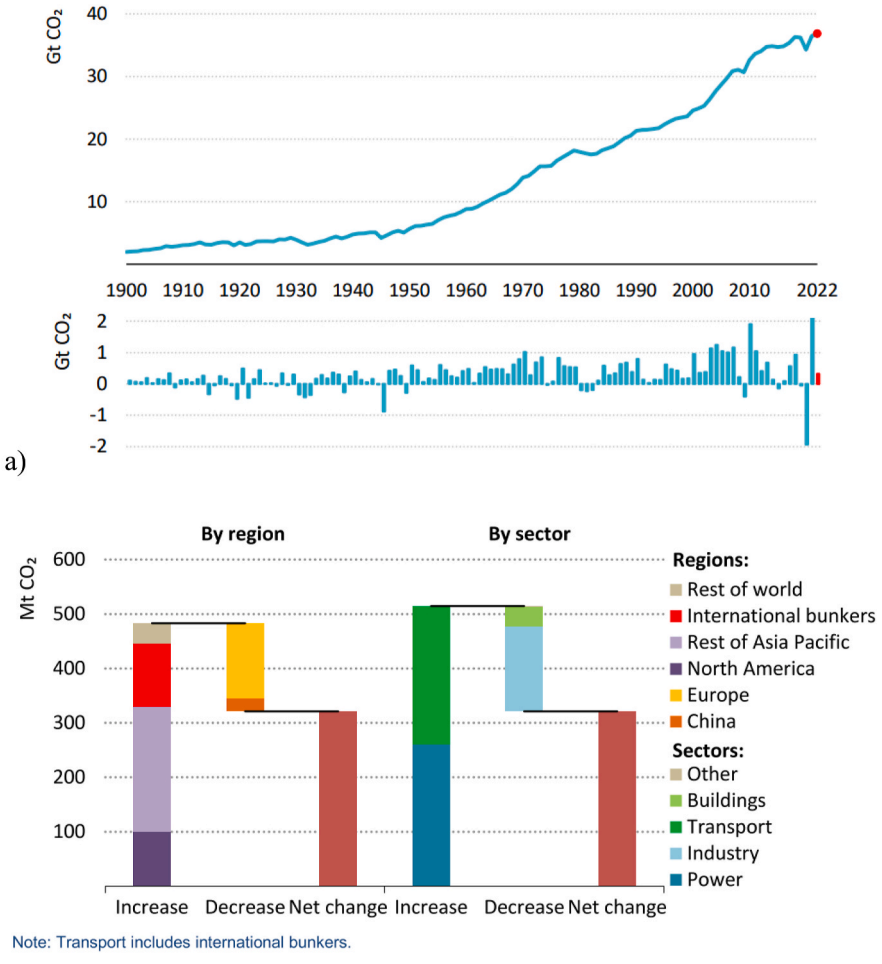

Fig. 1. CO_2 emissions: a) global from industrial processes and energy combustion from 1900 to 2022, b) change in CO_2 emissions by region and by sector, 2021–2022 [1].

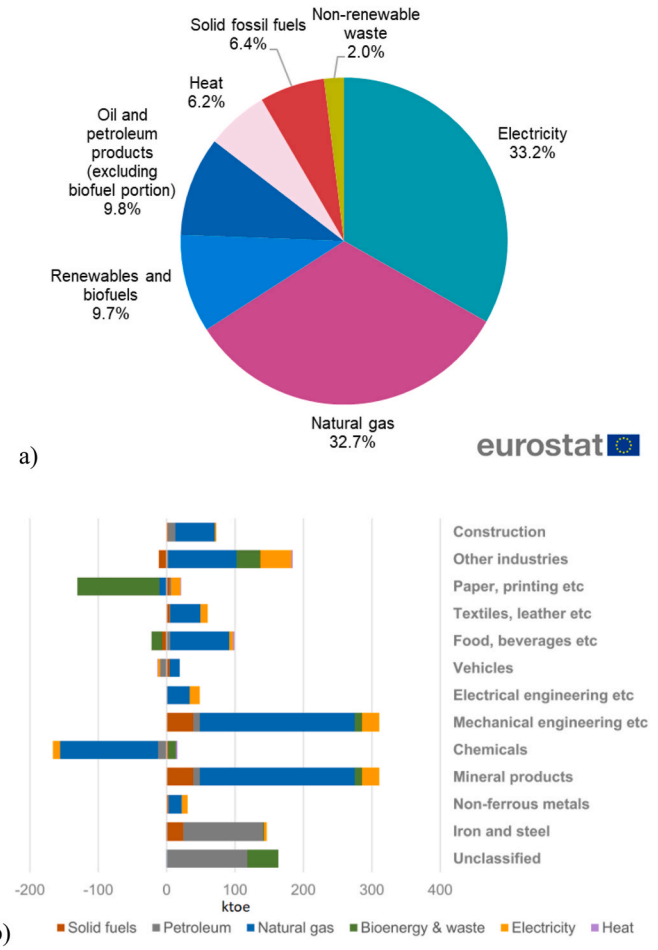

Fig. 2. Energy products used in industrial sector: a) EU in 2021 [4], b) change in industrial consumption sub-sectors from 2020 to 2021 by fuel in UK [5].

been a comprehensive review of research work on the modelling of vapour compression high-temperature heat pumps with an indication of the software that can be used. Numerical modelling allows a significant reduction in the time and cost involved in optimising HTHP systems compared to experiment. It is therefore important to be aware of the possibilities offered by simulation software as well as the assumptions or simplifications made in different programmes. This article provides a comprehensive overview of the solutions used for HTHP modelling and highlights the differences between the various simulation tools and identifies those that meet the requirements for HTHP. However, in order to understand the difficulties arising from modelling high-temperature pumps, the individual sections focus on: Section 2 provides a basic description of the principle of HP and a breakdown of the HTHP of pumps operating in sub- and *trans*-critical systems. Section 3 and 4 provides a broad description of the cycle configurations and the possible refrigerants to be used in HTHPs. Section 5 reviews HTHP modelling approaches and software that can be employed. Thus, covers the scientific gap regarding HTHP modelling. Additionally, the paper provides an overview of heat pump potential applications in various sectors.

2. Heat pump fundamentals

. Heat pumps can be of various designs and for waste heat recovery they can operate as compression, absorption or hybrid compression-absorption heat pump [10]. This article focuses on vapour compression high-temperature heat pumps that use the thermodynamic cycle to transport energy. These are devices that extract heat from the source: air, water, ground or industrial processes and transfer it to the refrigerant in the hot heat exchanger (evaporator). The stored energy in the working fluid is then transported to the cold heat exchanger (condenser), where it is released. The working fluid used to transport this heat in vapour compression heat pumps occurs in two different phases [7]. The reverse Carnot cycle is the theoretical cycle that consists of the following phases: The evaporator is one of the four components of a heat pump along with the compressor, condenser and expansion valve, Fig. 3A. Heat transfer from the environment to the refrigerant takes place during the isothermal process 4-1. In the evaporator, heat is extracted from the environment into the refrigerant during the 4-1 isothermal process. The evaporated refrigerant enters the compressor. In a reverse Carnot cycle, an isentropic process takes place during which the refrigerant is compressed adiabatically 1–2. The refrigerant is then isothermally condensed under pressure in the condenser and the heat is transferred to the heat sink 2–3. The refrigerant is transported to the expansion valve where an isentropic expansion process takes place and the working fluid is adiabatically expanded 3–4 after which the cycle repeats, Fig. 3B. The presented Carnot HP cycle, also known as a refrigeration cycle, consists of reversible processes that are impossible to apply to real-world systems. Consequently, the majority HPs are based on a vapour compression cycle (the reverse Rankine cycle) where isenthalpic expansion rather than isentropic occurs, Fig. 4 [7,9]. Adamson and al [9] stated that from a heat transfer point of view, the irreversibility of the compression and expansion processes in real vapour compression cycles means that its Coefficient of Performance (COP) will not be higher than 60 % of the COP of the Carnot cycle, with the same sink and source temperatures [9]. However, it is possible with an efficient compressor and low pressure drop heat exchangers to go above 60 %.

There are a number of methods for classifying HTHP: temperature ranges, cycle configurations including cascaded cycles. Two heat pump cycles are considered below: a subcritical cycle, where heat is released below the critical temperature and pressure of the refrigerant during condensation, and a *trans*-critical cycle, where heat is released above that point, as indicated by the red dot C in Fig. 5. In a *trans*-critical cycle, heat rejection does not take place via the condenser but via the gas cooler by single-phase sensible cooling. Due to the fact that the temperature glide in this case is significantly greater than in the condensation process, Austin and Sumathy [11] point out that this cycle is more favourable for applications requiring a large temperature rise (heating applications). In a *trans*-critical CO_2 system, there are large pressure differences between the heat absorption pressure and the heat rejection pressure, and therefore large thermodynamic losses occur during the expansion process. Therefore, expansion work recovery device may additionally be used in this type of system.

In subcritical cycles, the expansion device works most efficiently when the refrigerant enters it as a single phase (fully condensed as a saturated or sub-cooled liquid). The appearance of gas during expansion (gas flash) reduces the COP and the heating and cooling capacity [11].

To prevent this, heat pumps can be optimized by using sub-cooling the liquid after the condenser [7]. Additional components of the HTHP system such as flash tanks, sub-cooler, economiser, ejector or internal heat exchanger are discussed in the context of refrigerants in Section 3.

3. Heat Pump cycle configurations

High-temperature heat pumps are influenced by several key parameters. These encompass the temperature of the heat source, the temperature of the heat sink, the temperature lift, the type of refrigerant utilised, and the efficiencies of individual components, among others. These factors can be further categorised into subgroups, including both system design and operating conditions. Numerous research endeavours have been undertaken to enhance the Coefficient of Performance of HTHPs, achieved through the strategic optimisation of these factors.

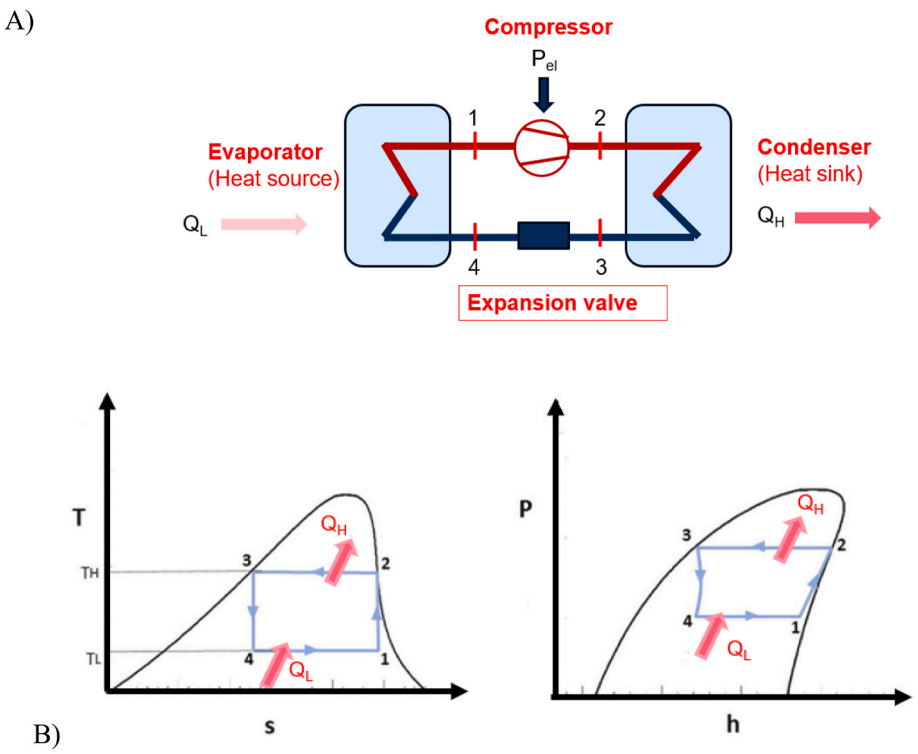

Fig. 3. Reverse Carnot cycle diagram (A), with T-s and P-h diagram (B).

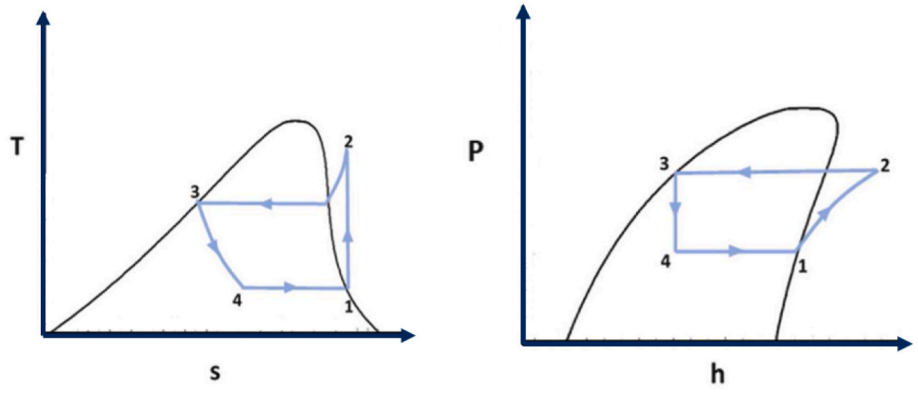

Fig. 4. Reverse Rankine vapour compression cycle: T-s and P-h diagram [9].

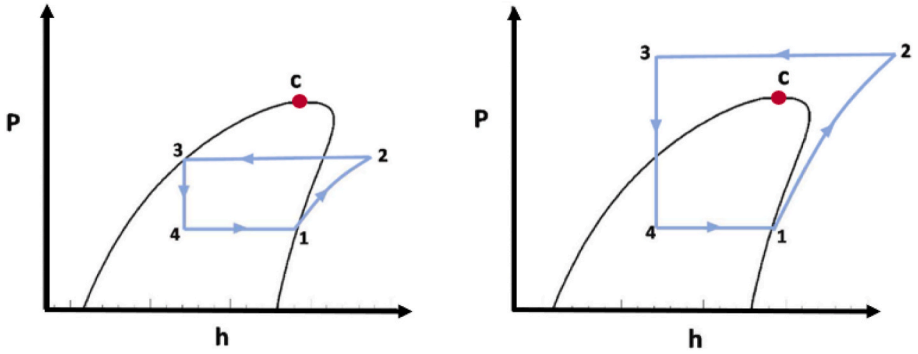

Fig. 5. Pressure-enthalpy HTHP diagrams: a) subcritical cycle, b) *trans*-critical cycle.

3.1. Coefficient of performance

Coefficient of Performance defined as the amount of heat transferred to the heat sink divided by the amount of work done by the compressor expresses the thermodynamic efficiency of the HP system. Arpagaus et al. [6] determined that temperature lift is one of the major impacting factors. This represents the difference between the heat source and heat sink temperatures. Typically, the COP of a HTHP decreases with increased temperature lift. This can be justified by the Carnot COP, where the numerator is the absolute temperature of the heat sink and the denominator is the difference between the absolute temperatures of the heat sink and source. Thus, the HP Carnot COP decreases with increasing temperature lift and increases with increasing temperature of the heat sink. In Ref. [6], several HTHPs were reviewed and compared in terms of their COPs. Regarding the temperature lift effect, the authors reported that the COP varied between 2.4 and 5.8 at temperatures lift of 95 and 45K, respectively. Considering a constant heat sink temperature (120 °C), the highest and lowest COPs were achieved at lift temperatures of 30 and 70K, with corresponding values of 5.7–6.5 and 2.2–2.8. Verdnik and Rieberer [12] explored the capabilities of an R600 (n-butane) HTHP, designed to harness waste heat in a temperature range of 40 °C–60 °C. This HTHP was used to supply temperatures ranging from 110 °C in sub-critical mode to 160 °C in *trans*-critical mode. Their investigation delved into the impacts of various internal and external parameters on both COP and heating capacity. The study drew on data gathered from both the physical prototype and a simulation model. In the sub-critical operating mode, a heating capacity of 30.7 kW was achieved, along with a COP of 4.4. These results were obtained with a heat source inlet temperature of 60 °C, elevating the heat sink temperature from 80 °C to 110 °C. Transitioning to the *trans*-critical mode further enabled the system to attain a heat sink outlet temperature of 160 °C, providing a heating capacity of 24.2 kW at a reduced COP of 3.1. In Ref. [13], a water vapour twin-screw compressor with water-injection was designed and a vapour compression very high-temperature heat pump (VHTHP) prototype was built. The primary objective of this experimental investigation was to generate a high-temperature output. The experimental findings revealed that, as the condensation temperature rose from 111 °C to 150 °C, the COP of the VHTHP decreased from 6.10 to 1.96, at an evaporation temperature of 85 °C. The peak COP of approximately 6.1 was achieved with a heating capacity of 285 kW at evaporation and condensation temperatures of 85 °C and 117 °C, respectively. Furthermore, this study reported that the maximum attainable condensation temperature for the water vapour-based VHTHP was 150 °C, yielding a COP of 1.96. At identical temperature lifts, a positive relation between the COP and the output temperature was achieved. This observation underscores the VHTHP's suitability for applications demanding higher output temperatures while maintaining a consistent temperature lift.

Numerous studies have been conducted on cycle enhancements for high temperature heat pumps through the adoption of additional components or modified configurations specifically for improved performance.

3.2. Advances in subcritical vapour compression cycles for HTHPs

The main cycle arrangements have been classified differently by authors of other review papers on HTHPs. In this paper, the cycles are discussed based on the similarities and differences between the HP configurations studied. The component features analysed in each of the reported cycles, alongside the key operating and performance metrics, are presented in Table 1.

The simplest standard vapour compression cycle, described in Section 2, has been investigated using a range of fluids but has mostly been limited to lower temperature applications of around 60 °C–80 °C [26–28]. Heat sink temperatures are closely linked to temperature lifts (the difference in temperature between the heat sink and heat source), and thereby high temperature lifts are generally associated with a high temperature application. Standard cycles with single stage compression tend to be limited by the pressure ratio across the compressor, which in turn dictates the anticipated temperature lift. Conventional cycle configurations have a maximum lift range between 30 °C and 80 °C, with most cycles achieving a temperature rise closer to the lower end of the spectrum. However, standard cycles are still appealing due to their simplicity, implying potential cost savings, as well as for preliminary experimental studies to assess working fluid performance and application suitability. Zhang et al. [14] developed a single-stage heat pump test system in Tianjin University using a scroll compression unit, to evaluate the performance of a novel near azeotropic ecological mixture (BY-5) with a critical point of 155 °C and 43.7 bar; they also used the acquired experimental data to validate a model for prediction. Their test results show that BY-5 has a potential use for lifting available heat sources at 70 °C–80 °C to sinks reaching 130 °C, where the obtained COP is over 3.0 for lifts lower than 46 °C [14]. Another near-azeotropic refrigerant mixture named BY-4 (T_c = 150.2 °C, P_c = 44.4 bar) was examined experimentally in a single stage vapour compression cycle with similar temperature limits as in Ref. [14] and achieved COPs above 3.5 for temperature lifts of over 30 °C, with the maximum heating capacity (122 kW) and COP (3.61) obtained at a heat source temperature of 110 °C [15].

Flash tanks (FTs), acting as a type of a liquid/vapour separator, have been implemented in rigs of standard cycles by researchers using water (R718) as the working fluid [13,16,17]. Heat pumps with flash tanks have been shown to be more economic and efficient in comparison to those with sub-cooler (SC) economisers (ECs) because flash vessels ensure that the inlet vapour to the compressor is close to saturation which reduces compression work [29]. The numerical and experimental

Table 1
Performance overview of subcritical HTHP cycle configurations found in literature.

Ref.	Year	E/S	Refrigerant	T_{source}/T_{evap} [°C]	T_{sink}/T_{cond} [°C]	COP [−]	Standard	SS + FT ± IHX	SS + EC/SC ± IHX	SS + IHX	SS + EJ + IHX	MS + IHX	MS + EC + IHX	MS + FT	MS + FT + IHX
[14]	2017	E	BY-5	70–80/-	110–130/-	3.1–2.57	✓								
[15]	2014	E	BY-4	-/50–70	80–110/-	5.67–1.32	✓								
[16]	2014	E	R718	86–94/-	-/118–122	4.5–5.5		✓							
[17]	2019	E	R718	-/83–87	-/120–128	5.0–3.8		✓							
[13]	2020	E	R718	/75–85	-/111–150	6.1–1.9		✓							
[18]	2012	E	ECO3	-/35–60	-/80–140	1.0–5.0			✓						
[19]	2017	S	various	80/-	160/-	3.68–4.58			✓			✓			
[20]	2020	S	various	40–100/-	100–140/-	1.7–6.0	✓			✓				✓	
[21]	2019	S	various	-/25–50	-/105–125	2.3–6.0				✓	✓	✓			
[22]	2020	S	various	-/80	-/140	1.0–4.5			✓	✓	✓				
[23]	2020	S	R245fa	65/-	110–140	4.5–2.5									✓
[24]	2015	S	various	80/-	160/-	4.53–4.94							✓		
[25]	2021	S	R245fa	30–90/-	100–140/-	1.0–10.2			✓	✓	✓	✓	✓		✓

test results produced by Chamoun et al. [16] are in agreement and therefore inferences were based on the outcomes of the parametric studies performed under steady-state and dynamic modelling. Similarly, in 2019 Wu et al. [17] conducted experimental tests on a water HTHP with evaporation temperatures of 83 °C and 87 °C; COPs of 3.89 and 4.4 were achieved for condensation temperatures of 121.8 °C and 121.4 °C, respectively, with a compressor power input of around 54 kW at a compression ratio of ≈4 for a 194 kW heating capacity. When the condensing temperature increased to 125.5 °C and 126 °C, the system's COP dropped to 3.6 and 4.03 respectively. Simulation results of the same work showed condensation temperatures reaching 160 °C can be achieved with a COP of 2.19 and a high compression ratio of 13. In the following year, the same group used their test facility to showcase results for condensation temperatures up to 150 °C at the cost of a threefold increase in compression ratio, a linear rise in power consumption, and significant reductions in heating capacities and COPs (to 1.9) as the condensation temperature increased from 110 °C to 150 °C [13].

A new refrigerant, ECO3, with no publicly declared information on composition and properties besides a GWP of 980 and a B1 safety group, has been used as the working fluid in a demonstration for an industrial heat pump supplying hot water with evaporation and condensation temperatures of 35 °C — 60 °C and 80 °C — 140 °C, respectively [30]. Experimental findings from the standard single-stage cycle with an internal heat exchanger and a sub-cooler indicated a COP of approximately 4.5 and energy efficiencies in the range of 55 % — 65 % with evaporation temperatures below 50 °C and condensation temperatures below 100 °C (temperature lifts around 60 °C); higher sink temperatures and lifts induced considerable losses caused by the poor performance of scroll compressors operating at the imposed high pressure ratios [30]. This conclusion coincides with the benefit of having a sub-cooler to obtain high COPs for medium to low temperature lifts, whereby the sub-cooler cools the liquid refrigerant leaving the condenser, further leading to an increased heat capacity and a reduction of throttling flash gas [18]. The internal heat exchanger placed between the outlets of condenser and evaporator acts to raise the compressor discharge temperature (as the suction temperature of the compressor increases), assisting in the attainment of a higher sink temperature at the cost of increased compression work [9].

Multi-stage compression is used to increase compressor efficiency, compression ratios and temperature lifts [31]. Most of the time it is essential to have multi-stage compression as it may not be practically possible to achieve the required pressure ratio in a single stage. Fukuda et al. [19] considered a cycle configuration similar to that in Ref. [30] without the sub-cooler to compare the performance of HFOs R1234ze(Z) and R1233zd(E) with HFC R365mfc. The highest COP (4.24) and lowest compression ratio (5.94) and irreversible losses (7.48 kW) for the single-stage cycle were obtained with R1234ze(Z) for a waste heat temperature of 80 °C and a heat sink temperature of 160 °C [19]. The authors investigated the performance of a two-stage compression cycle with multiple condenser units and an internal heat exchanger, which for the same conditions and working fluid as the single-stage cycle, showed an improvement of around 8 % in COP and slightly lower component irreversible losses through the use of more than one condenser for heat extraction [19]. Likewise, Kosmadakis et al. [20] compared the performance and economics of three cycle arrangements using three low GWP refrigerants; they summarise their proposed cycles for a range of temperature lifts based on both performance and cost criteria. They suggested that the two-stage cycle with a flash tank and an open intercooler is the most efficient but not cost-effective, and that R1234ze(Z) is the most suitable refrigerant for performance measures, except for low temperature lifts; the main issue however is the limited commercial readiness of that particular HFO [20].

The use of ejectors (EJs) to enhance vapour compression cycles has been increasingly researched due to their simplicity and ability to recover expansion work [32] that would be lost through the throttling process, which reduces losses and compressor work, and thereby raises COP [33]. Bai et al. [21] analysed the performance of three ejector-based heat pumps using a range of sustainable working fluids. The combination of the condenser outlet split ejector-based cycle with R1233zd(E), in contrast with other arrangements, showed the most promising improvements in terms of compressor size reduction by almost 10 %, plus COP and exergy efficiency improvements by up to 12 % and 40 % respectively [21]. Mateu-Royo et al. [22] evaluated the use of an ejector-based cycle, an economiser with a parallel compression cycle, and a single-stage cycle using multiple refrigerants, all with internal heat exchangers to improve performance. In comparison with the single-stage configuration, R245a in the ejector cycle showed about a 40 % increase in both the COP and the volumetric heating capacity, but the cycle with the highest COP was the one employing parallel compression [22].

Hao et al. [23] looked at the position of an internal heat exchanger in a two-stage vapour compression cycle with a flash tank to overheat the refrigerant pre-compression and undercool it post-compression; their two suggestions of forward reheating and rear reheating is based on the placement of the IHX before the first expansion valve or before the second expansion valve, respectively. Their simulation results, carried out in Aspen Plus [34] indicated that the forward reheating structure requires a higher compressor power input whereas the rear reheating cycle allows for elevated heat absorption in the evaporator and a better COP compared with a single-stage configuration.

Multi-stage (MS) extraction cycles have been the focus of several researchers to reduce expansion and exergy losses in the throttle and condenser. Cascade cycles, like multi-stage compression and expansion cycles, are a combination of vapour compression cycles linked through a cascade heat exchanger representing the evaporator for the topping cycle and the condenser for the bottoming cycle. A study of four such cycle arrangements (tandem/series, cascade, and multi-stage cycles) has been published by Kondou et al. [24] for temperature limits of 80 °C and 160 °C. The cascade cycle with R1234ze(Z) and R365mfc gives a relatively high COP (up to 4.94) and allows other refrigerant combinations and lubricants to be investigated [24]. As per the studies on low GWP refrigerants presented in Subsection 4.3, the same ISTENER group has recently performed a thorough analysis of a wide range of cycle configurations using over ten working fluids/working fluid combinations for heat sink temperatures up to 140 °C [25]. While some cycles appear to be more complex than traditional ones, the economic analysis conducted seems to convey that even the two-stage cycles including extra components are cost-feasible with significant improvements in COP [25].

3.3. *Trans*-critical high temperature heat Pump cycles

Trans-critical heat pumps operating at pressures above the critical point function in the same manner as the subcritical heat pumps, but heat rejection takes place through sensible cooling in a gas cooler rather than through phase change in a condenser, allowing for interdependency between the temperature and pressure. Given that the gas cooler temperature glide in *trans*-critical cycles is higher than that in the subcritical counterpart, closer matching of that difference and the heat sink temperature is required to reduce thermodynamic losses. Generally, *trans*-critical cycles are used for applications requiring a high temperature lift but at lower pressure ratios than subcritical cycles, hence allowing for better compression efficiency. Several reviews on *trans*-critical heat pumps, particularly using carbon dioxide as a working fluid, have been published but they are not limited to high temperature applications [9,11,35,36]. In fact, the review of experimental research on *trans*-critical cycles suggests that heat to heat recovery (heat pump) systems are mostly relevant to the domestic water heating sector for their high temperature lifts and high volumetric heating capacity with maximum heat sink temperatures of 100 °C–120 °C [36].

Table 2 presents the performance overview of selected *trans*-critical

Table 2
Overview of experimental *trans*-critical HTHP cycle configurations in literature.

Ref.	Year	E/S	Refrigerant	T_{source}/T_{evap} [°C]	T_{sink}/T_{cond} [°C]	COP [−]
[37]	2019	E	R1234ze(Z)	82/-	150/-	3.32–3.72
[38]	2018	E	R600	80/-	180/-	3.5
[39]	2020	E	R600	40–60/-	110–160/-	3.1–4.5
[40]	2019	E	R744	5/-	115/-	3.5
[41]	2002	S	R744	−/−6.4–0.3	65–120/-	2.5–3.5
[42]	2018	S	R134a	-/20–35	113/-	2.5–4.7
[43]	2020	S	HFOs/HCs	30–80/-	200/-	2.6–3.5
[44]	2018	S	R744/R1234ze(Z)	50/-	-/90–100	4.6–3.3

high temperature heat pumps found in literature. R1234ze(E) was used in a standard cycle experimental setup for a heat sink temperature of up to 150 °C with a maximum COP of 3.72; the authors suggested that adding an internal heat exchanger and parallel compression could improve the performance of the *trans*-critical cycle [37]. Similarly, butane (R600) was tested in a standard *trans*-critical cycle employing two oil-free turbo compressors and a 300-kW capacity gas cooler, achieving COPs above 3.5 [38]. Butane with its overhanging two-phase region on the pressure-enthalpy diagram would require a high level of superheat prior to the compressor in a subcritical cycle to avoid wet-compression [9], however a *trans*-critical cycle can alleviate that requirement slightly. R600 was also investigated in both subcritical and *trans*-critical cycles by Verdnik et al. [39] using mostly off-the-shelf components. Subcritical conditions achieved the higher COPs, reaching 4.5 for a 30.8 kW capacity with a heat sink temperature of 110 °C (double the heat source temperature), whereas a maximum temperature of 160 °C was only obtained in the *trans*-critical operation but a reduced COP of 3.1 [39].

Natural refrigerant carbon dioxide (R744) has been the subject of various *trans*-critical cycles due to its low critical temperature compared to other common working fluids. Bellemo et al. [40] tested R744 in a HTHP prototype 90 kW *trans*-critical cycle for heating water from around 5 °C–115 °C using multiple copper-brazed gas coolers in series for spray drying processes; a compression ratio of approximately 3.7 was obtained using two CO_2 piston compressors. Modelling results from the early 2000s implied a comparable COP for an almost analogous *trans*-critical CO_2 cycle with an internal heat exchanger as a recuperator [41]. Comparing several refrigerants in a *trans*-critical cycle with a sub-cooler, Wang et al. [42] found that R134a showed optimal thermodynamic performance (COP and heat recovery ratio) as well as suitable economic benefits. Arpagaus et al. [43] inferred that *trans*-critical CO_2 HPs are not fit for high temperature industrial waste heat recovery applications, and recommend *trans*-critical cycles with parallel compression and internal heat exchange using R1233zd(E), R1224yd(Z) or R600 for delivering heat up to 200 °C. They indicated that the gas cooler pressure is the critical parameter that requires tuning to obtain good performance [43]. A simulated hybrid source HTHP with a *trans*-critical CO_2 cycle, absorbing heat from air, with a R1234ze(Z) subcritical cycle absorbing waste heat, showed a 24 % higher COP than a single source heat pump operating in the same environment for condensation temperatures reaching 100 °C [44].

3.4. Hybrid and multi-temperature heat Pump systems

Hybrid vapour compression/absorption heat pump cycles have been explored to overcome the challenges associated with single vapour compression cycles such as inflexibility and mismatching between heat source and heat sink temperatures. The absorption cycle usually employed for heat recovery from low-temperature sources can elevate the quantity of heat supplied to a hybrid heat pump [45]. The ammonia-water working fluid combination has been the most commonly used in such systems where the high-pressure water solution and ammonia vapour release heat in the absorber before being expanded, followed by a two-phase evaporation of ammonia in the desorption process [9]. Experimental results from R717/R718 hybrid cycles show COPs in the range of 1.5 — 2.5 and sink temperatures between 90 °C — 130 °C [46,47], whereas higher COPs between 3 and 4 are obtained in modelling studies [48,49].

Multi-temperature cycles are used to tailor a particular temperature application using multiple heat pump components, additional elements, as described in Subsection 3.2, and cascades to enhance performance. Arpagaus et al. [50] conducted a review on multi-temperature heat pumps; since 2016, three primary studies have been identified that present multi-temperature heat pumps with sink temperatures over 100 °C. The cycle with two evaporators, a booster compression and an economiser suggested by Mateu-Royo et al. [25] is the only one accounting for multi-temperature waste heat recovery from two heat sources; this cycle configuration, with one heat source temperature at 40 °C, shows improved performance for second heat source temperatures above 80 °C (up to 60 % increase in COP). The multi-evaporator/condenser cycles proposed by Fukuda et al. [19] and Kosmadakis et al. [20] also act as multi-temperature cycles with COPs around 4 at heat sink temperatures up to 140 °C.

4. Refrigerant selection

This section covers the configurations of high temperature heat pump systems encompassing available refrigerants and potential cycle arrangements.

Refrigerant selection is a key consideration for heat pump, air-conditioning, and refrigeration systems where it acts as the working fluid absorbing and rejecting heat through evaporation and condensation. The choice is primarily dependent on the system operating conditions (heating capacity, source and sink temperatures, and pressures). However, further ecological, commercial, and safety considerations, which are often conflicting, are necessitated by the application and environmental protection regulations. These constraints and the

Table 3
Requirements for refrigerant properties [6,11,51].

Property	Requirement
Pressure	Positive to avoid ambient moisture and air infiltration
Critical temperature	Relatively high for subcritical HPs so that condensation temperature is from critical point to avoid reduction in enthalpy of vaporisation for latent cooling Low for *trans*-critical HPs to operate over critical point and use gas cooler for sensible heat transfer
Critical pressure	Low to reduce design challenges and maintain compressor capability
Normal boiling point	Low for lower evaporation temperature and low volumetric flow rate for practical compressor sizes
Freezing point	Lower than HP temperatures
Specific heat ratio	Low for lower discharge temperature for improved compressor performance
Molecular weight	Low for compressors that perform better with high pressure and lower vapour specific volumes (reciprocating)
Thermal conductivity	High for improved heat transfer in evaporator and condenser
Viscosity	Low for high heat transfer coefficients and lower power input
Liquid density	Low for less refrigerant charge
Chemical congeniality	Compatible with component materials and lubricants (miscibility)
Toxicity	Low toxicity (A safety groups over B)
Flammability	Low flammability (lower numbers in safety index)
ODP (R11 = 1)	Low or no ODP to avoid release of atoms that destroy the stratospheric ozone layer which protects the earth from direct ultraviolet sun radiation
100-year GWP (CO_2 = 1)	Low to avoid absorption of infrared emissions from earth greenhouse gases
Availability	Readily or easily available
Cost	Low price for commercialisation

associated necessities are summarised in Table 3 based on various thermodynamic/thermo-physical, chemical, environmental, and commercial properties.

The critical point of the refrigerant plays a leading role in its appropriateness for HTHPs. The critical temperature (T_c) curbs the maximum temperature for subcritical cycles where at least 10–15 °C should be kept between the condensation temperature and the critical temperature [6]; condensation temperatures should be kept as far as possible below the critical point to make the most use of higher vaporisation enthalpies and thus higher COPs [52]. The emergence of *trans*-critical heat pump cycles, particularly with the use of CO_2 (R744) [11], has allowed some independence from the critical temperature where heat is recovered in a gas cooler instead of a condenser. The critical pressure (P_c) of the refrigerant should generally be low to avoid high working pressures for better compressor capabilities, even though high critical pressures are associated with high vapour densities, i.e., increased volumetric heating capacities, which might lead to more compact components. As for *trans*-critical cycles, pressures well above the critical point allow low gas cooler exit temperatures, which enhances performance [9].

The minimum pressure of the heat pump system should always be above atmospheric to avoid any fluid permeation from the surroundings [53]. Although high pressures yield smaller footprints, the upper pressure limit depends on compressor type but is usually around 20–25 bar for screw compressors [54] with reports of higher values for specific compressor/working fluid combinations. High pressures also dictate more rigorous metallurgical standards for component materials. Simultaneously, low compression ratios are preferable to lower the input work. Göktun [55] proposed that the selection criteria for the thermal properties of refrigerants for HTHPs are $T_c \geq 170$ °C, $P_c \leq 50$ bar, 25 °C $\leq$ NBP $\leq$80 °C, and 50 g/mol $\leq M \leq$ 150 g/mol.

Safety standards relate to refrigerant flammability and toxicity. According to ASHRAE Standard 34 [56] toxicity is characterised by classes A (lower toxicity) and B (higher toxicity), whereas flammability is categorised as classes 1 (no flame propagation), 2/2L (lower flammability), and 3 (higher flammability). It is worth noting that the safety of the system relates to its complexity and thus accompanying costs.

The ecological concerns of refrigerants arise from incidents of refrigerant leakages or accidents that would cause detrimental polluting effects. The environmental indices of concern are the ozone depletion potential (ODP) and the global warming potential (GWP). Other indicators used for assessing the sustainability of refrigerants are: the total equivalent warming impact (TEWI) accounting for the lifetime total direct refrigerant emissions as CO_2 equivalents and the indirect CO_2 emissions from the energy consumption of the whole system; and the life-cycle climate performance (LCCP) which constitutes TEWI and all refrigerant manufacturing emissions [57]. Fig. 6 depicts the progression of refrigerant types since their inception, from the highly toxic, flammable, and harmful chlorofluorocarbons (CFCs), to less damaging hydrochlorofluorocarbons (HCFCs), through to hydrofluoroolefins (HFOs) and hydrocholorofluorooelfins (HCFOs) for ozone concerns, reaching more sophisticated blends that target global warming and higher efficiencies; refrigerants have undergone significant development over the last 200 years [58]. Natural refrigerants and hydrocarbons (HCs) have been continuously used due to their availability and non-destructive properties, with worries about the safety of HCs. This section reviews the use of the aforementioned refrigerant types for HTHP applications, taking into account the main requirements.

Rarely do pure refrigerants qualify on all factors, whereas curated mixtures are able to provide the flexibility in achieving suitable thermodynamic properties while abiding by environmental regulations. Refrigerant mixtures come in three types [61]: azeotropic mixtures behave as a single substance that cannot be separated. The boiling point of an azeotrope is less than that of its constituents and they are mostly reserved for low-temperature refrigeration. Near azeotropic mixtures are similar to azeotropic ones but allow a larger collection of refrigerant choice and have a low temperature glide (temperature difference between evaporation and condensation). The refrigerant mixtures most suitable for HTHP applications are of the zeotropic type as they have a higher potential for improvements [53]; they deviate from the behaviour of pure substances completely during phase-change processes which means that they have a comparatively higher temperature glide leading to partial leakages of the volatile substances initially. Zeotropic mixtures can pose further complications for HTHP configurations where ideal vapour-compression cycles resemble the Lorenz cycle instead, but this challenge can be overcome by using a sophisticated mixture with suitable properties, and by better matching the temperature profiles during heat absorption and rejection [62].

4.1. Chlorofluorocarbons and hydrochlorofluorocarbons

Under the Montreal Protocol, commonly used CFCs in HVAC&R applications are banned due to their harmful environmental effects, and HCFCs are being fully phased out from both developed countries from 2020, and developing countries by 2030 [63]. With global warming potency over 2000 times that of carbon dioxide, such refrigerants would need to show very high-performance characteristics to even be contemplated, however, there are not many CFC refrigerants that are suitable for the high temperature demands of HTHPs. The most used refrigerant in domestic and automotive units R12 Freon has a relatively low critical temperature of 112 °C limiting its use for HTHPs. Other CFCs with properties that might have been suitable for HTHPs are listed in Table 4. CFCs such as R115 with $T_c = 80$ °C have been previously used for high temperature heating up to 70 °C [64]. Studies on CFC

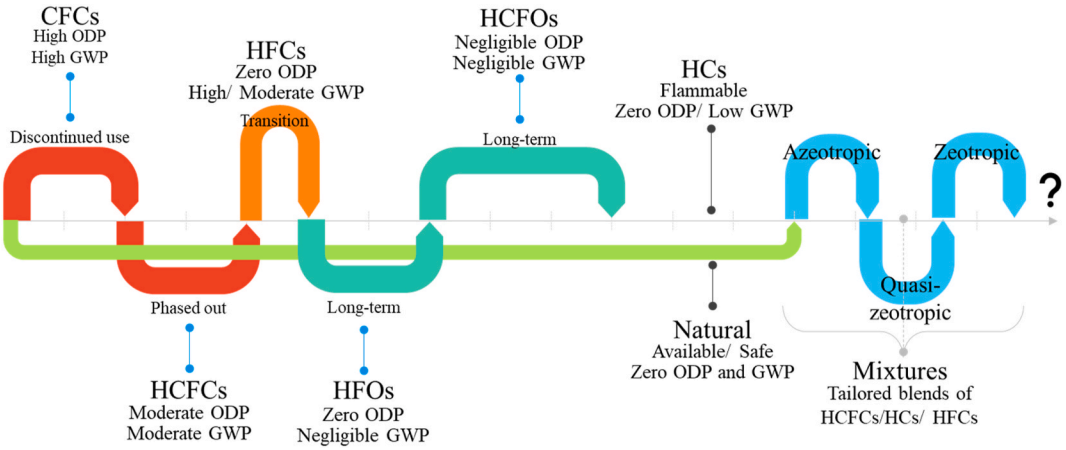

Fig. 6. Transitions of refrigerant types [59,60].

Table 4
Properties of selected CFC and HCFC refrigerants [6,53].

Refrigerant	M [g/mol]	T_c [°C]	P_c [bar]	NBP [°C]	ODP	GWP	Toxic	Flammability
CFCs								
R11	137.4	198.0	44.1	23.7	1	4000	No	No
R12	120.9	112.0	41.4	−29.8	1	10,600	No	No
R113	187.4	214.0	33.9	47.6	0.85	5820	No	No
R114	170.9	145.7	32.6	3.8	0.58	8590	No	No
HCFCs								
R123	152.9	183.7	36.6	27.8	0.03	79	Yes	No
R124	136.5	126.7	37.2	−12.0	0.03	527	No	No
R142b	100.5	137.1	40.6	−10.0	0.065	782	No	Low
R21	102.9	178.5	51.7	8.9	0.04	148	Yes	No

alternatives for HTHPs have been conducted since the early 1990s, but still with a limitation of temperature not reaching the 100 °C heat sink level [54,65]. The same can be inferred from the meagre array of HCFC refrigerants that are also included in Table 4. The other obvious drawback is that most HCFCs are either toxic or flammable [56]. Ongoing HCFC systems will have to be retrofitted with more ecological refrigerants which would require suitable substitution without sacrificing performance, or they will have to be decommissioned.

4.2. Hydrofluorocarbons

Due to their unfavourable environmental impact, CFCs and HCFCs were replaced by hydrofluorocarbons (HFCs) which have a lower global warming effect as indicated in Table 5 [65]. R245ca seems to be a likely candidate due to its good performance and improved environmental capacities alongside a high critical temperature and a good miscibility with polyester lubricants [66]. The more toxic R245fa has been evaluated for HTHPs in the dyeing industry up to 97.8 °C by Wu et al. [67]; their measured data showed COP values up to 3.9. HFC mixtures have also been investigated for substitution in older CFC/HCFC systems but have shown higher discharge temperatures that would affect the compressor life [51]. R152a/R125 at mass percentage 85:15 has been reported to have a critical temperature of 106.2 °C but has only been studied for lower temperature domestic applications [68]. Kobe Steel developed their "HEM-90A″ two-stage heat pump with a twin-screw compressor for heating water up to 90 °C using the HFC mixture R134a/R245fa; with a 10 °C water temperature lift from 80 °C, a COP of 2.8 has been achieved for 176.2 kW heating capacity [69]. Other zeotropic mixtures with critical temperatures over 170 °C have also been established [6].

Given that HFCs still have a significantly high GWP (>10), they are deemed transition refrigerants, due to be phased out possibly before HTHPs markets gain stronger traction.

4.3. Hydrofluoroolefins and hydrochlorofluorooelfins

Hydrofluoroolefins, some of which are presented in Table 6, were introduced as unsaturated HFCs with zero ODP and much lower GWP indices. R1234ze(Z) has been suggested as a substitute for R245fa [70], and R1234ze(E) [71] or R1336mzz(E) [72] for R134a for high temperature applications due to similar thermo-physical properties and negligible GWP. Kondou and Koyama [24] conducted a numerical thermodynamic performance assessment of four HTHP cycle configurations using HFO refrigerants, to replace or in conjunction with HFCs, for pressurised water heating up to 160 °C from a heat source of 80 °C. Their results show that a cascade cycle of HFO-R1234ze(Z) and HFC-R365mfc gave the highest COP range of 4.3–4.94; it is important to note the health hazard and instability of R365mfc [73]. Yan et al. [74] simulated a simple HTHP VCC with several working fluids for condensation temperatures between 70 °C and 110 °C. Notably, the HFOs R1234ze(Z) and R1234ze(E) demonstrated good performance in comparison to HFCs with COPs reaching 3.61; additional cycle modifications could possibly make the COP higher. Longo et al. [75] investigated the condensation behaviour of R1234ze(Z) experimentally alongside other HFC and hydrocarbon (HC) refrigerants, where the studied HFO exhibited much larger heat transfer coefficients and relatively low pressure drops due to friction.

Hydrochlorofluorooelfins (HCFOs) have also been hailed as alternatives to refrigerants with high global warming potential. The two most studied HCFOs are R1224yd(Z) and R1233zd(E), listed in Table 6. The use of R1233zd(E) in HTHPs to recover waste heat at 50–80 °C and supply hot water up to 160 °C was theoretically analysed by Jiang et al. [78] who concluded that the heating capacity and COP ranges of a system with two-stage compression and vapour injection are 2.09 MW–4.23 MW and 2.70–2.93, respectively, depending on the temperature lift, for high temperature operation. Frate et al. [79] established that the most efficient working fluids out of a selection of HFOs and HCFOs are the ones with a low volumetric heating capacity but that R1233zd(E) offsets that with COPs as high as 6.0 using a single-stage compression for a condensing temperature up to 150 °C. Similarly, Bai et al. [21] simulated several refrigerant candidates where R1233zd(E) delivered high COP (3.74–5.90) and exergy efficiency (around 60 %), particularly in a condenser outlet split ejector-based cycle for heat condensation above 105 °C. For a 110 °C condensing temperature, Alhamid et al. [80] showed numerically that R1224yd(Z) achieved COPs in the range of 2.74–4.75, and R1233zd(E) attained similar values for evaporation temperatures of 50 °C–70 °C in a HTHP cycle with two-stage compression. A lab-scale HTHP single-stage system, with an internal heat exchanger (IHX), operating with R1233zd(E), was developed in Switzerland where a COP of 2.43 was achieved for a baseline

Table 5
Properties of selected HFC refrigerants [6,55].

Refrigerant	M [g/mol]	T_c [°C]	P_c [bar]	NBP [°C]	ODP	GWP	Toxic	Flammability
R134a	102.0	101.1	40.6	−26.1	0	1300	No	No
R152a	66.1	113.3	45.2	−24.0	0	138	No	Low
R227ea	170.0	101.8	29.3	−15.6	0	3350	No	No
R236fa	152.0	124.9	32.0	−1.4	0	8060	No	No
R244ca	150.5	221.0	37.1	54.8	0.02	N/A	No	Low
R245ca	134.0	174.4	39.3	25.1	0	716	No	No
R245fa	134.0	154.0	36.5	14.9	0	858	Yes	No
R365mfc	148.1	186.9	32.7	40.2	0	804	No	Low

Table 6
Properties of selected HFO and HCFO refrigerants [6,9,76,77].

Refrigerant	M [g/mol]	T_c [°C]	P_c [bar]	NBP [°C]	ODP	GWP	Toxic	Flammability
HFOs								
R1234ze(E)	114.0	109.4	36.4	−19.0	0	<1	No	Low
R1234ze(Z)	114.0	150.1	35.3	9.8	0	<1	No	Low
R1336mzz(E)	164.1	137.7	31.5	7.5	0	18	No	No
R1336mzz(Z)	164.1	171.3	29.0	33.4	0	2	No	No
R1243zf	96.1	103.8	35.2	−26.5	0	<1	No	Low
HCFOs								
R1224yd(Z)	148.5	155.5	33.3	14.0	0.00012	<1	No	No
R1233zd(E)	130.5	166.5	36.2	18.0	0.00034	<1	No	No

heat sink temperature of 110 °C and a temperature lift of 50 °C [81]. In recent years, the ISTENER university research group in Spain has performed several studies on HFOs and HCFOs [82–85] for moderately high temperature applications. This refrigerant sub-group seems to be one that is here to stay and dominate the HTHP market due to its thermodynamic performance qualities plus the satisfactory environmental and safety characteristics.

4.4. Hydrocarbons and natural refrigerants

Hydrocarbons (HCs) and natural working fluids have been used in refrigeration systems from their advent mainly due to their wide availability and cheap prices. Heavy HC refrigerants in Table 7 with critical temperatures over 100 °C are suitable for high temperature applications, with butane (R600) and iso-butane (R600a) being the preferred working fluids for very high temperatures. Bamigbetan et al. [86–88] extensively evaluated and reviewed HTHPs working on natural and HC refrigerants. The numerical analysis of a cascade system with propane (R290) and R600 used for water heating from 95 °C to 115 °C gave a COP of 2.6 for a 370-kW heating capacity [89]. Similar results were achieved experimentally for an almost identical cycle configuration and refrigerant selection for a 20 kW HP [90].

The obvious hurdle for HCs is their high flammability. HFC/HC mixtures have been investigated for a possible suppression of the flammability related to HCs, and the oil incompatibility of HFCs [51]. There are several noteworthy mixtures with critical temperatures over 100 °C, with the highest T_c of 124.5 °C for R124/R142b/R600a (90:08:02 by mass) [51]. Nonetheless, such mixtures continue to have high GWPs which make them incongruous for the long run. HC mixtures have been used in heat pumps to replace CFCs and HCFCs, though not many studies have been accomplished for high temperature applications. However, the mixtures R290/R600a (45.2:54.8 by mass) and R290/R600 (60:40) have critical temperatures of 117.5 °C and 118.7 °C, respectively [51], with no ODP and a GWP of 20 which makes them feasible choices for certain HTHPs. Research on refrigerant mixtures for industrial heat pumps has been prominent in China as discussed in Ref. [92].

Two out of the three natural working fluids set out in Table 7 resolve the major non-thermodynamic predicaments linked to refrigerant selection (environmental compliance and safety). While ammonia (R717) does have satisfactory ecological properties, it presents itself with health hazards [79], a high compressor discharge temperature [93], and material limitations [88]. Water (R718) has an extremely high critical temperature making it a tempting option for HTHPs. Nevertheless, given the high normal boiling point of 100 °C, systems require operation in sub-atmospheric pressures for heat sources lower than its NBP. In addition to that, the low vapour density of R718 means that high pressure ratios imply very large or high-speed compressors, increasing its existing complications with material and lubricant compatibility. A HTHP substituting natural gas boilers for 180 °C heat production was simulated using R717 and R718; both fluids show enhanced theoretical performance in comparison to R290, but this does not remove the compressor design issues of each. It has been reported that centrifugal compressors for water are suited to overcome the size and speed challenges [94,95]. The only refrigerant discussed in this paper with a critical temperature lower than 100 °C is carbon dioxide (R744); it also has another special property which is the high operating pressure, though not as high as those for R717 and R718. While R744 has excellent environmental operational properties, like lower pressure ratios, elevated heat transfer properties, high volumetric capacity, and compatibility with materials/lubricants [53], making it suitable for domestic cooling and heating, its critical point conditions substantially circumscribe CO_2 from being using in typical sub-critical HTHP cycles. However, there has been lots of research activity on the development of *trans*-critical cycles with CO_2 [9,35,96]. Dai et al. [97] found COP values up to 4.85 in their assessment of a *trans*-critical CO_2 HTHP cycle for industrial heat upgrade with dual-temperature evaporation and an ejector. Further performance metrics using CO_2, and other refrigerants are presented in the upcoming section as part of the cycle configurations.

Table 8 summarises the main advantages, challenges and proposed solutions of the refrigerant types presented in this review. It also proposes some future research directions based on the current state-of-the art of HTHP systems.

5. Modelling software for heat pump systems

There are many approaches that can be used to describe and model the behaviour of heat pumps. Each of them will require a different degree of detail with regard to the input parameters. This section covers software for modelling heat pump systems. According to the literature

Table 7
Properties of selected HC and natural refrigerants [6,9,76,77,91].

Refrigerant	M [g/mol]	T_c [°C]	P_c [bar]	NBP [°C]	ODP	GWP	Toxic	Flammability
HCs								
R600	58.1	152.0	38.0	0.5	0	4	No	High
R600a	58.1	134.7	36.3	11.8	0	3	No	High
R601	72.2	196.6	33.7	36.1	0	5	No	High
R601a	72.2	187.2	33.8	20.2	0	5	No	High
Natural								
R717	17.0	132.3	113.3	33.3	0	0	Yes	Low
R718	18.0	373.9	220.6	100.0	0	0	No	No
R744	44.0	31.0	73.8	56.5	0	1	No	No

Table 8
Summary of refrigerant characteristics [88].

Refrigerant	Merit	Challenges	Solutions	Future direction
CFCs	Experience	High GWP	Substitutes	Discontinued
HCFCs	Experience	High GWP Toxic/Flammable	Substitutes	Accelerated phase-out Retrofitting
HFCs	Good performance Lubricant compatibility	High GWP	Mixtures	Transition to environmentally friendly refrigerants
HFOs	Low ODP	Relatively low T_c	HCFOs	Further development of new refrigerants
HCFOs	Low ODP High T_c Good performance Material/lubricant compatibility	Limited choice Relatively expensive Relatively new	Commercialisation Testing with different cycle arrangement	Manufacturing of new refrigerants
HCs	Availability Environmentally friendly	Flammable High discharge T High discharge P	Safety measures	Mixtures Lubricant/coolant research Development of compressors for HCs
Natural: CO_2	Suitable for *trans*-critical HTHPs Low ODP/GWP	High gas cooler temperature Expansion losses Low T_c High discharge P	Matching of temperature glide using heat exchanger optimisation Expanders Set lower discharge pressure than optimum for HTs	Ejector research Compression improvement
Natural: R717	Wide use	Material compatibility High discharge P High discharge T Toxic	Steel and aluminium instead of copper Suitable intercooler/de-superheater integration	Focus on enhancement for moderately high temperature HPs Use in cascade systems with other refrigerants
Natural: R718	Availability High T_c	Incompatible with carbon steel Low vapour density High discharge T	Stainless steel Multi-stage compression Turbo-compressors	IntercoolingTechnology improvement

review the following approaches can be specified: computational methods, simulation programmes that allow dynamic simulations, design models [98].

The first group is derived from standards EN 15316-4-2. This method for describing the performance of heat pumps has changed considerably over the last 16 years. Initially in 2007, the focus was on the simplified seasonal performance method (SSPM) under steady state condition or on the bin method based on component efficiency data and outdoor air temperature. SSPM focused on the heating season and the typology of a system where the tabulated values of fixed heat pump performance classes were used. Anything not covered by test data such as part-load or on-off operation was not taken into account in this standard [99]. In 2017, changes were made to allow thermal efficiency and COP to be determined at both full load and part load based on standards EN 14511 series or EN 14825, respectively. Both approaches are hourly methods and assume an exergy concept. The thermodynamic process is described by the exergy efficiency in which the numerator is the actual COP of the process, and the denominator is the ideal Carnot COP. Due to varying compressor efficiencies in real systems, the description of the heat pump performance with this method (constant exergy efficiency) will depend on the number of available test points. Thus, the applicability of this methodology is limited to well described system solutions.

In the second group, which includes simulation software that performs dynamic simulations of energy systems, TRNSYS and EnergyPlus, among others, are commonly used. TRNSYS allows the analysis of transient systems in a user-friendly way through its graphics-based development environment [100]. Furthermore, it enables the modelling of dynamic systems beyond the typical performance evaluation of thermal and electrical energy systems. As noted by Zanetti et al. in Ref. [101] the various components of the system are linked together and presented as "Types", black box models. Bordignon et al. [102] presented a water-to-water heat pump model, for single-stage and cascade configurations in two modes of cooling and heating using a new type of TRNSYS developed in FORTRAN. Connections to some REFPROP 10.0 [103] subprograms have been included to reflect the thermodynamic properties of the selected fluids. The authors presented diagram of how the developed model works because, as they pointed out, TRNSYS uses a commercial heat pump performance matrix for HP simulation, which is linked as external files using software such as Engineering Equation Solver (EES) or Microsoft Excel. Energy Plus works in a similar way [101,102]. In this programme, the performance of the heat pump can be integrated using the curve fitting method [104]. Lu and Ziviani [104] created quasi-steady-state models of heat pumps using EES to obtain an efficiency map. Along with this, they used the efficiency-NTU model (lumped method) to describe the internal heat exchanger in the EES models. In their work, they compared eight scenarios with different types of heat pumps: ground source heat pumps, vapour compressor two-stage heat pumps for cold climates, dual-fuel heat pumps and membrane heat pumps. By design, EnergyPlus is not a black box [105]. Worldwide access to the source code means that anyone can improve the programme and enhance its accuracy. Shen et al. in Ref. [106] presented an air source integrated heat pump (ASIHP) model in EnergyPlus in which they used indicators and performance curves from the ASIHP prototype. The above findings were confirmed by Weck-Ponten et al. in Ref. [98]. In their study they compared the most commonly used heat pump modelling software. They paid attention to.

- the type of model: black box (BB), grey box (GB), characteristic curve (CC);
- mathematical description: parameter estimation-based (PE); equation-fit (EF); physical (PHY);
- type of source/sink medium: air (A); brine (B); water (W);
- transient effects of heat exchanger (yes: x; partly: (x))
- possibility of modelling the refrigeration cycle (yes: x; partly: (x))
- capacity control (yes: x; partly: (x))

The results of their analysis are presented in Table 9.

Both approaches presented for modelling heat pumps relate to solutions where the sink temperatures are below 100 °C. High temperature heat pumps require a more precise approach due to the operating temperature parameters, the type of refrigerant or the type of compressor used. To model HTHP operation, one of the following tools presented in Table 11 should be used. The physical-based HTHP model approach is considered. This enables the optimisation of the HP or its individual components both at refrigerant cycle level and component geometry or geometrical relationships between components [98,107]. NIST

Table 9
Results of the analysis carried out in Ref. [98].

Simulation program/ library	Model type	Mathematical description	Type of source/sink medium	Transient effects of heat exchanger	Model the refrigeration cycle	Capacity control
Polysun	BB	CC	A/W, B/W, W/W			
MATLAB	BB	CC	B/W			
TRNSYS	BB	EF	A/W, B/W, W/W	(x)		
Energy Plus	BB	EF	W/W			
IDA ICE	BB	EF	B/W	(x)		
OpenGeoSys	BB	EF	B/W			
INSEL	BB	EF	A/W, B/W			
GLHEPro	BB	EF	W/A			
Modelica/AixLib (heat pump)	GB	EF, PE	A/W, B/W, W/W	x	(x)	x
MATLAB	GB	PE	A/W, B/W, W/W	(x)	x	
html online	GB	PE	B/W, W/W		x	x
EnergyPlus	GB	PE	W/W		x	
EES IMST ART	GB	PE	W/W		(x)	
EES	GB	PE	B/W	(x)	(x)	x
IDA ICE	BB	PE	W/W			
Modelica/Buildings	GB	PE	W/W	x	(x)	x
INSEL	GB	PHY	A/W, B/W, W/W		x	

Reference Fluid Thermodynamic and Transport Properties Database (REFPROP) is most commonly used to describe refrigerant properties in accordance with Table 10 [84,101,108–110]. The programme allows the calculation of thermophysical properties of selected pure liquids and their mixtures [111]. Dynamic link library (DLL) enables researchers to work with other programs or languages such as Excel, MATLAB, LabView, FORTRAN, Python, C++, Mathematica [112]. The COP and the cost and size of the HTHP compressor are significantly influenced by the volumetric heating capacity (VHC) of the working fluid. Therefore, C. Arpagaus et al. [6] verified by simulation the thermodynamic efficiency of selected refrigerants as the most suitable for systems with a single-stage subcritical heat pump cycle with an internal heat exchanger. For this purpose, the researchers used Engineering Equation Solver to determine VHC, COP and pressure levels for a condensing temperature range of 60–200 °C. EES [113] has a database of transport and thermodynamic properties of many substances and enables the numerical solution of thousands of coupled integral, differential and non-linear algebraic equations. Hong et al. [114] presented a new model of variable refrigerant flow in the heat pump. Compared to the models included in Energy Puls, the proposed solution allows consideration of advanced control of variable condensing and evaporation temperatures, detailed heat loss calculations in refrigerant pipes, and the possibility of reducing the number of performance curves to improve model accuracy and usability.

Most HTHP models presented in the literature consist of a detailed description of each of the components used: compressor, condenser, expansion valve, evaporator, refrigerant and other components [11,97]. This modelling approach was presented, among others, by Hassan et al. in Ref. [107] who proposed five stages of the global modelling method and described each in detail, Fig. 7, not forgetting the parametric studies. The model concerned high temperature heat pumps integrated into pumped thermal energy storage systems with discharge temperatures below 160 °C and sink temperatures above 60 °C. Dai et al. [97] collated the energy equations for each component for five HTHP CO_2 systems taking into account compressor, gas cooler, evaporator, throttling valve and ejector which plays a key role in 4 of the 5 cycles presented. Two possible model types have been specified for ejectors: the constant-pressure mix

ing model, and the constant-area mixing model. The authors chose the constant-pressure mixing ejector because of its stable performance over a wide range of backpressures. Austin and Sumathy [11] have developed a model for a *trans*-critical carbon dioxide heat pump system and also focused on each of the HTHP components individually. Examples of assumptions for high-temperature heat pump models are shown in Table 10. Table 11 provides an overview of the tools used for HTHP modelling.

Chamoun et al. [16] presented vapour compression systems based on screw compressors that reach sink temperatures of 130–140 °C with water as refrigerant. The model developed in Modelica integrates the finite volume and moving boundary (FV-MB) method to account for the presence of non-condensable gases in the heat exchangers. Additionally, the moving boundary concept between phases for flash evaporation and purging models was covered. It has been stated that complicating the model by specifying each phase separately does not significantly increase the accuracy of the results. Therefore, homogeneous flow being in thermal equilibrium was assumed. Wu et al. [17] developed a mathematical model of a water vapour HTHP system with sink temperatures of 120–130 °C and temperature lift 40K. The models comprised twin-screw water vapour compressor model with water injection, flash tank, falling film, evaporator, expansion valve. The first of these models uses the efficient and multi-stage compression model. Due to the energy conservation of the expansion valve, the specific enthalpy of the water vapour remains the same. Heat losses to the surroundings are neglected. Dai et al. [119] presented different heat transfer models for calculating the heat transfer coefficient for a single-stage and two-stage compression system, boiling and condensation.

Although the heat pump operates under varying conditions, most models assume steady-state conditions for the system. Therefore, it is advisable to extend the analyses to include the dynamic performance of HTHP systems, taking into account the performance of the operation during the shutdown and start-up stages. Defining the flow as homogeneous, and assuming thermodynamic equilibrium, allows strong mixing to be ensured throughout the heat exchanger operation without degrading the accuracy of the results [16].

6. Applications, environmental impact and cost for end users of high temperature heat pumps

6.1. Applications

As reported in Arpagaus et al. [6], high-temperature heat pumps have the potential to be used in various applications, including hot water supply, plastics, textiles, wood, construction, beverages, cement, food, paper, metal, energy storage, and chemical industries. Fig. 8 shows possible heat sources for HTHPs in industry. The applicability of HTHPs in the different sectors depends mainly on the sink temperature. In other words, as the sink temperature of the heat pump increases, the range of applications the heat pump can be used in also increases. Although heat pumps may not be able to supply the required temperature for certain industries, they are still beneficial in providing a substantial portion of

Table 10
Example assumptions for individual HT heat pump components.

	General assumptions	Compressor	Condenser	Evaporator	Expansion valve	Other components
[11]	*Trans*-critical CO_2 cycle. Steady-state conditions Heat loss in connecting piping: negligible Changes in potential and kinetic energy: negligible	Operates adiabatically The isentropic and volumetric efficiency: estimated	Operate adiabatically		Expansion process is isenthalpic	Gas cooler: concentric tube counter flow heat exchanger model. For an evaporator and a gas cooler, the heat transfer and energy balance equations are similar
[97]	Steady-state conditions for dual- temperature evaporation CO_2 HTHP Heat loss of each component: negligible	semi-hermetic reciprocating	Pressure drops in heat exchangers negligible Pinch point temperature difference 5 °C		Ejector efficiency: constant One-dimensional steady state fluid flow	Specific enthalpies of the refrigerant before and after the throttling valve: equal Saturated state of the refrigerant from the outlet of the evaporator and separator
[17] MATLAB (validated model)	Steady-state conditions Pressure drops are negligible (in pipes, condenser, evaporator, flash tank). Heat losses to the environment are negligible (in the condenser, evaporator, flash tank and compressor). Change of gravitational and kinetic energy of the water vapour and water are negligible. Pressure and temperature of water vapour and water are homogeneous respectively at any instant in the control volume. Between water vapour and water no pressure difference and temperature difference	The multi-stage compression model Efficient model Mass flow rate of water vapour compressed based on the mass balance The volumetric efficiency 0.9925 Isentropic efficiency 0.6	Finite volume method Newton's cooling law and overall heat transfer coefficient are used	Model of falling film evaporation assumptions: Dispenser evenly dispenses. Refrigerant vapour - saturated and gas-liquid interface is in thermal equilibrium. Heat transfer of liquid membrane includes nuclear boiling in the liquid membrane and convection evaporation at the Force of the refrigerant-not considered. Along the direction of pipe length the performance of the falling film evaporator taken into account The full liquid zone in 0.75 % of the pipe and 0.25 % in the falling film zone.	Specific enthalpy of water vapour: constant	Refrigerant: Heat transfer coefficient taken from the literature Flash tank: Water vapour sucked into the compressor equal the water vapour produces in the flash tank
[16]	One dimensional flow Viscous dissipation is negligible Uniform flow and in thermodynamic equilibrium	Steady-state conditions Volumetric and isentropic efficiency supplied by the compressor manufacturer	Generic approach suitable Presence of non-condensable gases in heat exchangers addressed by using the formulation of the moving boundary and finite volume. Dry air in the heat-exchanger (perfect gas)		Isenthalpic expansion, negligible: mechanical inertia of the working fluid, thermal inertia of the valve and heat losses, no mass accumulation	The purging valve model: ISO 8878 standard The two-phase flash separator and purging system: mass and energy conservation
[107] IMST-ART	Steady-state conditions Inside refrigerant lines and heat exchanger no pressure drop Constant pinch point of 5K	Constant compressor efficiency 0.65 Constant compressor heat losses 25 %,	Always saturated liquid at condenser outlet of heat exchangers is discretized numerically (finite volume method) For the wall temperature: the semi-explicit method Pressure drop and heat transfer included One-dimensional flow assumed Evaporator capacity of 40 kW -constant	Electronic and thermostatic expansion valves: constant superheat assumed Pressure drop and heat transfer: included	Refrigerant: R-1233zd(E) Flow: Pressure drop and heat transfer (-NTU method): included	

the required heat. While there are currently no reports or practical studies covering the use of HTHPs in all the aforementioned applications, numerous investigations are currently underway to accelerate developments in this field to raise the sink temperature, which would in future make HTHPs useable in their full range of potential applications.

Schlosser et al. [121]. analysed different HTHPs at various technology-readiness levels in a milk drying system. Here, the CO_2 *trans*-critical cascade heat pump showed the best performance, reaching a supply temperature of 210 °C with a COP of 2.14. This was followed by Stirling heat pumps and market available HTHPs, with corresponding COPs of 1.6 and 1.41. The latter heat pump exhibited a drying temperature of ~127 °C. Based on the economic study, the authors reported

Table 11
The tools used for HTHP modelling.

Soft	Cycle type	T_{source} °C	T_{sink} °C	COP	Refrigerant	Compressor type	Ref
Mathematical model	Subcritical vapour compression cycle	70–80	135	2.775-2.6	BY-5	Hermetic scroll compressor	[14]
Engineering Equation Solver (EES) Heat transfer analysis: logarithmic mean tem perature difference (LMTD) method	Subcritical single-stage cycle; Single-stage cycle with an IHX; Two-stage cycle with flash tank with open intercooler	40–100	140	1.7-3.2	R1234ze(Z), R1233zd (E) R1336mzz(Z)	semi-hermetic screw compressor	[20] S/E
Performances mapping and endurance tests	Subcritical two compression stages with closed economiser	80 50	140 100	4.43 4.48	ECO3TM	scroll compressors	[30] S/E
Engineering Equation Solver (thermodynamic equations) REFPROP 10.0 (thermophysical properties of each refrigerant)	Subcritical: • Single-stage cycle • Single-stage cycle with ejector • Two-stage cycle cascade • Two-stage cycle with economiser and flash tank • Two-stage booster cycle • Two-stage extraction cycle	30–90	100–150	1–6	HC-601, HFO-1336mzz(Z), R-514A HC-600 HC-600a HCFO-1233zd(E) HCFO- 1224yd(Z)	NA	[25] S
Mathematical model	Hybrid sources heat pump *Trans*-critical CO2 cycle	50	100	4.26-4.4	R1234ze(Z) CO_2	NA	[44]
Mathematical model	Subcritical: • a triple tandem cycle, • two-stage extraction cycle, • three-stage extraction cycle, • cascade cycle	70–130	100–60	4.3–4.94	R1234ze(E) R1234ze(Z) R365mfc	NA $\eta_{overall} = 0.61$-0.7	[24]
Engineering Equation Solver (thermodynamic equations)	Hybrid absorption–compression HP	80–100	200	–	ammonia–water mixture	NA $\eta_{is} = 0.8$, $\eta_{vol} = 0.90$	[49]
Engineering Equation Solver	*Trans*-critical vapour compression cycle	25–30	>110	3.85	R134a	$\eta_{motor} = 0.95$	[42]
Engineering Equation Solver	1 One-stage cycle with IHX 2 Two-stage cycle with economiser and IHX 3 Two-stage cycle with flash tank and IHX	40–90	154–189 116–125 103–148	1. 3.72-3.98 2. 3.82-3.99 3. 3.91–4.03	R1336mzz(Z) R1233zd(E) R1224yd(Z) R1234ze(Z) R365mfc R245fa	$\eta_{is} = 0.7$	[115]
Mathematical model:	Two-stage NH_3 heat pump system with closed intercooler CO_2 heat pump with IHE CO_2 heat pump with second IHE	0	100	1.5	CO_2	$\eta_{is} = 0.7$	[116] [117]
Mathematical model: component performance equations + Peng–Robinson equation: thermo-dynamic properties of CO_2.	*Trans*-critical CO_2 heat pump	65	120	3.4	CO_2	$\eta_{is} = 0.7$	[41]
Aspen Plus V9 (Thermodynamic Model)	Quasi-two-stage compression system with a two-stage expansion system (with flash tank and IHE)	60	120	3.6-4.5	R245fa	$\eta_{is} = 0.9343–0.04478 * \lambda p$ $\eta_{mechanical} = 0.83$ (λp- pressure ratio)	[23]
MATLAB: condenser: effectiveness-NTU method	Single-stage cycle with IHE	55–85	80–120	3.1–11.5	ammonia/R134a	reciprocating compressor	[118]
MATLAB	Water vapour compressor cycle with flash tank, liquid collector, a circulating water pump and an injection water pump.	80–90	120–130	3.64-4.87	water	Twin-screw water vapour compressor with water injection $\eta_{volumetric} = 0.9925$ $\eta_{is} = 0.6$,	[17]
IMST-ART Microsoft Excel regression tool	Subcritical cycle with subcooler and thermal energy storage	40–100	130	4–4.3	R-1233zd(E) is	Single piston compressor	[107]
1. Dynamic Modelling Laboratory (Dymola) 2. TIL library for modelling thermal systems 3. REFPROP 9.1 - refrigerant thermodynamic properties	Subcritical vapour compression cycle	60–100	100–125	<3.5	R600 R600a R601 R601a R1234ze(E) R1234ze (Z) R1233zd(E) R1336mzz(Z)	piston compressor with	[108]
Engineering Equation Solver REFPROP 10- refrigerant thermodynamic properties	Subcritical single-stage cycle Subcritical single-stage cycle with IHX	45–75	115–145	–	HFO-1336mzz(Z), HCFO-1233zd(E) HCFO-1224yd(Z)	reciprocating compressor $\eta_{electromechanical} = 0.95$	[84]
Engineering Equation Solver REFPROP- refrigerant thermodynamic properties	Subcritical: single-stage cycle single- stage cycle with IHX two-stage cycle	80 80 50,70,90 –	140 110 150 110, 130	2.23 3.41	HCFO-1233zd(E) HCFO-1224yd(Z) HFO-1336mzz(Z), HCFO-1233zd(E) n-	scroll compressor	[109]

(*continued on next page*)

Table 11 (*continued*)

Soft	Cycle type	T_{source} °C	T_{sink} °C	COP	Refrigerant	Compressor type	Ref
	two-stage cycle with IHX two-stage cycle with intermediate-IHX				Pentane HFO-1336mzz(Z), HCFO-1233zd(E), Butane n-Pentane		
Engineering Equation Solver REFPROP- refrigerant thermodynamic properties	Subcritical vapour compression cascade cycle with IHX in both stages	30,45,60	145	3.15	low-stage: HFO-1234yf, HFO-1234ze(E), butane, isobutane, propane high-stage: HCFO-1233zd(E), HFO- 1336mzz(Z), HCFO-1224yd(Z), pentane	reciprocating compressors	[110]

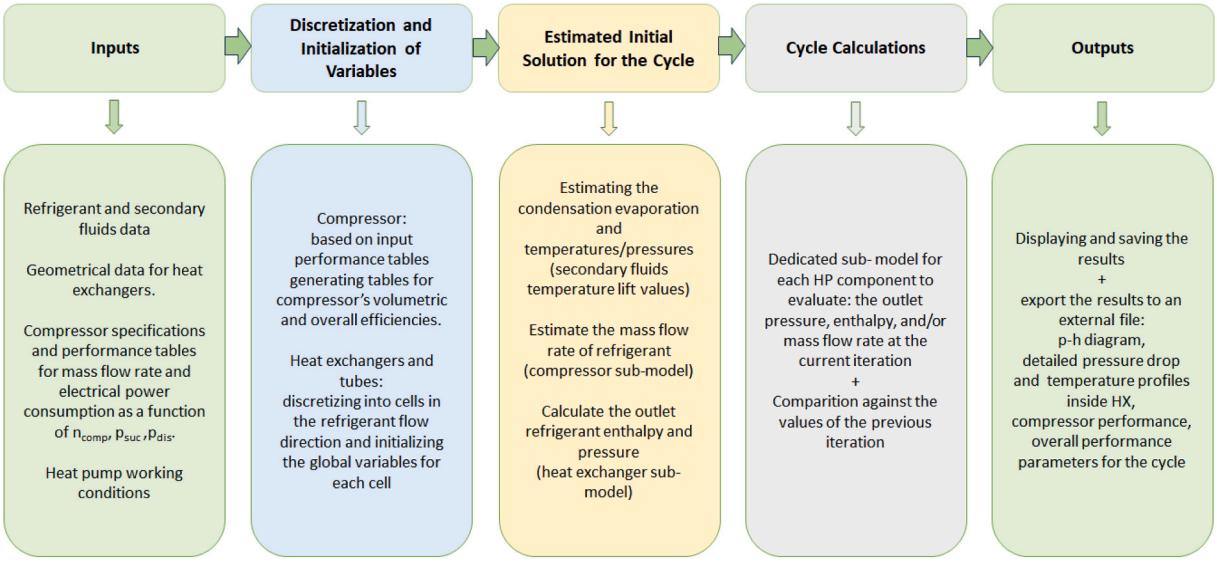

Fig. 7. Flow chart for HTHP global modelling [107].

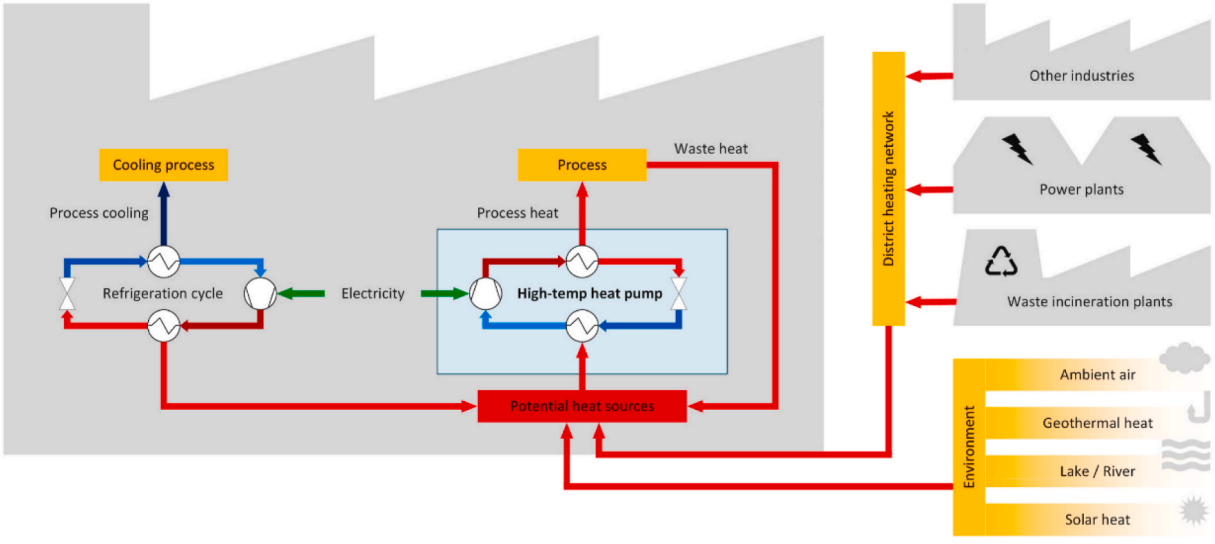

Fig. 8. HTHP potential heat sources in industry [120].

break-even point at electricity-to-reference-fuel price ratios of 1.56, 1.2, and 1.41 for the *trans*-critical, Stirling, and market available HTHPs, respectively. Walden et al. [122] designed an integrated system comprising a HTHP, thermal energy storage (TES), and a wind turbine. This system was able to provide heat for a steam generator that was connected to a steam consumer factory. The HTHP consumed electricity that was supplied by the wind turbine and the grid and, in turn, the HTHP supplied heat to the TES. The waste heat from the consumer factory was recovered by the HTHP, where it was subsequently used as a heat input to the cycle. Obrist et al. [120] presented a novel modelling framework including energy and material flows to study the potential of HTHPs in different industrial sectors in Switzerland. According to their findings, HTHPs are economically feasible up to a temperature of 150 °C. Furthermore, it is expected that by 2050, Switzerland has the economic potential to utilize ~900 MW in the food sector and ~100 MW in the paper industry. Fig. 9 shows the temperature ranges for HTHPs depending on the industry sector and the process involved.

6.2. Environmental impact

Heat pumps run using electricity. It is estimated that in 2023, the increase in renewable electricity capacity was almost 50 % more than in 2022 [124]. The current energy mix in all major markets means that heat pumps are seen as better for the climate than heating directly powered by fossil fuels. It is evident that the increase in renewable, low or zero carbon sources electricity generation increases the emission savings from heat pumps. According to the IEA report on The Future of Heat Pumps, in the global transition to sustainable and safe heating, heat pumps, which are powered by low-emission electricity, are a pivotal technology. Heat pumps compared to a gas boiler reduce greenhouse gas emissions by at least 20 %, taking into account today's refrigerants, even when powered by electricity with high emission levels. In countries with cleaner electricity, this reduction can be as high as 80 % [125]. Gaur et al. [126] points out that large-scale deployment of heat pumps on the demand side of the electricity grid is a major technological challenge and reflects the challenges of large-scale deployment of renewables. They also highlighted that further research and analysis is required to reduce the peak to average demand ratio. Tveit et al. [127] conducted a life cycle assessment comparing the environmental impact of high-temperature heat pumps, oil boilers, and natural gas boilers. To perform this comparison, a non-dimensional eco-indicator was used. Here, each point represents 1000th of the average European resident's annual environmental impact. This indicator was divided into four effective primary categories, namely human health, ecosystem quality, climate change, and resources. The HTHP showed the lowest indicators in all categories, with an overall eco-indicator of ~14, while the values for oil and natural gas boilers were around 30 and 27, respectively. The selection of refrigerants plays a pivotal role in determining the environmental impact of high-temperature heat pumps. Choosing environmentally friendly refrigerants can significantly reduce greenhouse gas emissions and contribute to a more sustainable and eco-friendly heating and cooling technology as discussed in section 4. In this context, Alhamid et al. [80] conducted an analysis to assess the environmental impact of R1224yd and R1233zd in comparison with R245fa in HTHPs. Their analysis was based on the total equivalent warming impact, which takes into consideration two types of emissions that are related to energy consumption and leakage. These were referred to as direct and indirect emissions. Both proposed refrigerants exhibited significant reductions with regard to influence on the environment, with direct emissions being reduced from 206 to 0.2-tonne CO_2 eq. Additionally, the indirect emissions were also reduced from 81.88 to 80.96 and 79.58 tonne CO_2 eq. for R1233zd and R1224yd, respectively. Another environmental analysis was carried out by Li et al. [128]. This analysis aimed to compare an integrated industrial waste heat recovery system that comprised a HTHP and a gas separation device with the conventional low-pressure steam employed in refinery processes. According to their findings, significant emissions reductions were achieved considering an operation of 8000 h per year. The highest annual reduction was reported for carbon dioxide, with a value of 3348 tonnes. This was followed by sulphur dioxide and nitrous oxides that had corresponding values of 101 and 50 tonnes, respectively.

6.3. Financial cost for consumers

The investment cost of a high-temperature heat pump (HTHP) is usually calculated per unit of energy, as it varies according to the required heat output. In other words, investment costs are defined by the size of the heat pump. According to Arpagaus et al. [6], the specific investment cost of HTHPs ranges between €250/kW and €800/kW. In Kosmadakis et al. [20], the techno-economic aspects of HTHPs used for recovering waste heat were investigated. Here, the HTHP was designed to generate heat at temperatures up to 150 °C from heat sources initially below 100 °C, employing both single- and two-stage cycles. The goal was to determine the most cost-effective approach across various combinations of heat sink and heat source temperatures. The findings revealed that the specific equipment cost of the heat pump typically falls within the range of €150/kW to €300/kW and is primarily influenced by the cycle design and operating temperatures. Furthermore, the discounted payback period for industrial installations displayed a wide range and could be as short as 3–4 years. It was concluded that, in terms of economic performance, the single-stage cycle with an internal heat exchanger is generally preferred, except in cases where there is a substantial temperature lift exceeding 50 K, where a two-stage cycle showed superior cost-effectiveness. Urbanucci et al. [129] demonstrated the relationship between the break-even cost of a high-temperature heat pump (HTHP) investment and the coefficient of performance (COP) of the HTHP when integrated into a trigeneration system. They found that with an assumed HTHP investment cost of €800/kW, the COP of the HTHP must exceed 2.9 for the proposed system to be economically competitive compared to separate production methods. In Dai et al. [119], the concept of cascade heating was presented, and five configurations of cascade heating HTHPs were considered and optimized to efficiently utilize waste heat. The findings indicated that cascade heating HTHPs offer significant advantages in terms of energy consumption, carbon and pollutant emissions, life cycle cost (LCC), and payback period (PBP). Regarding the economic performance over the system's lifespan, the LCC of the cascade heating flash tank superheated suction system (CFSUS) could be lowered by 4.5 %–18.3 % compared to conventional HTHPs. Furthermore, the PBP of CFSUS was the shortest at 3.1 years, representing a 15.4 %–65.9 % reduction compared to conventional HTHPs. However, the cascade-heating water cooled saturated suction system (CWSAS) was recommended, as the most suitable configuration, due to its superior overall energy, environmental, and economic performance. The authors published a flow chart to identify the economic, environmental and energetic performance of the HTHP system under study, Fig. 10.

7. Conclusions

High-temperature heat pumps enable operation under industrial conditions. They make it possible to recover heat from one production process and transfer it to the same or another process, but at a higher temperature level. This reduces the need to use fossil fuels, which will contribute directly to reducing greenhouse gas emissions. This is more significant if the electricity used to power the heat pump is coming from low or zero carbon sources. HTHPs are therefore becoming the future of various industrial sectors and further development should be pursued. High-temperature heat pumps which have a sink temperature above 100 °C are summarised in this paper under four aspects: cycle configurations, working fluid, modelling approaches, and applications. The types of refrigerant fluids that can be used in HTHP are discussed, as well as their environmental impact. From the literature review it appears that

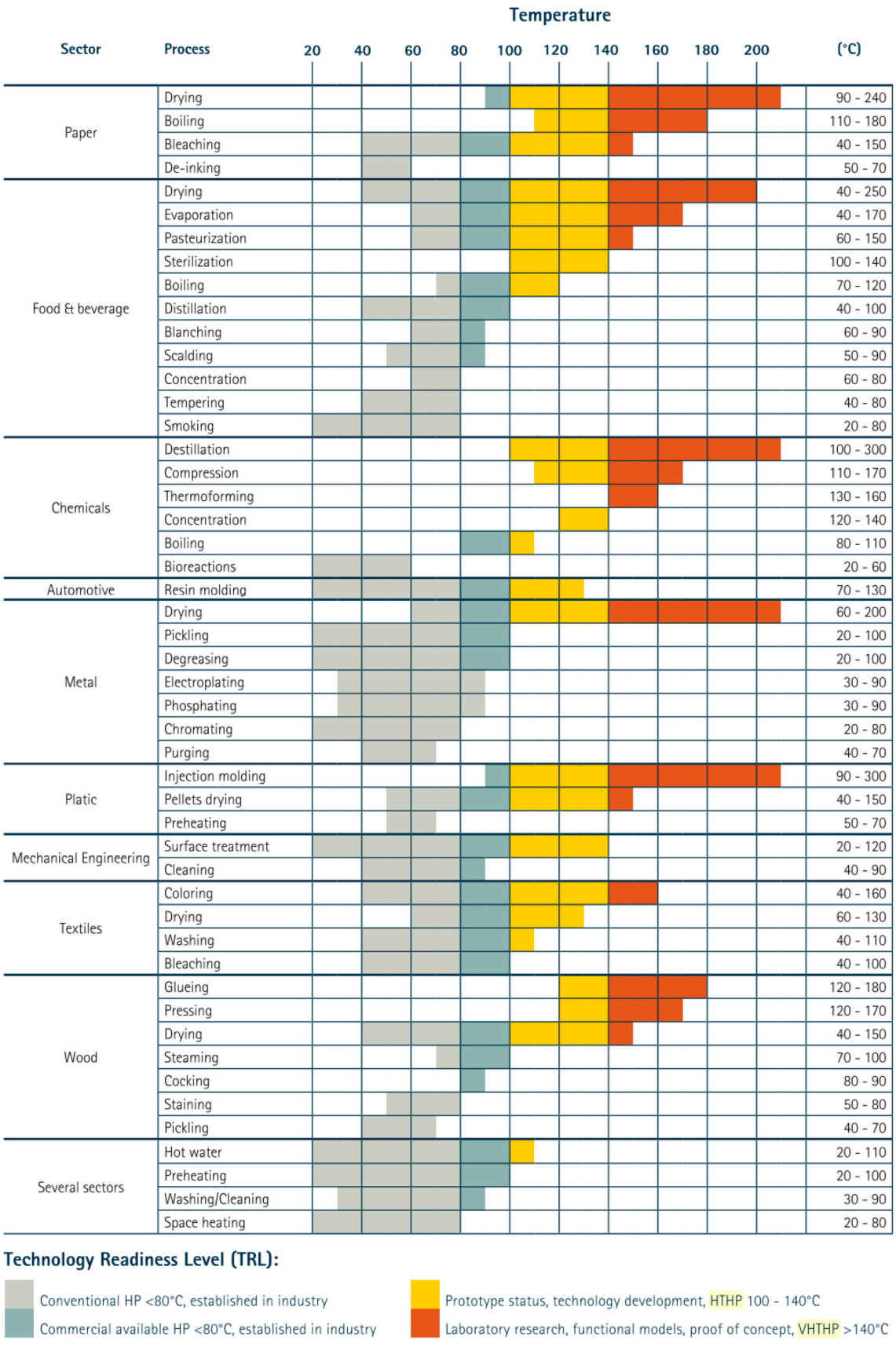

Fig. 9. Temperature ranges for industrial processes in different sectors of industry [123].

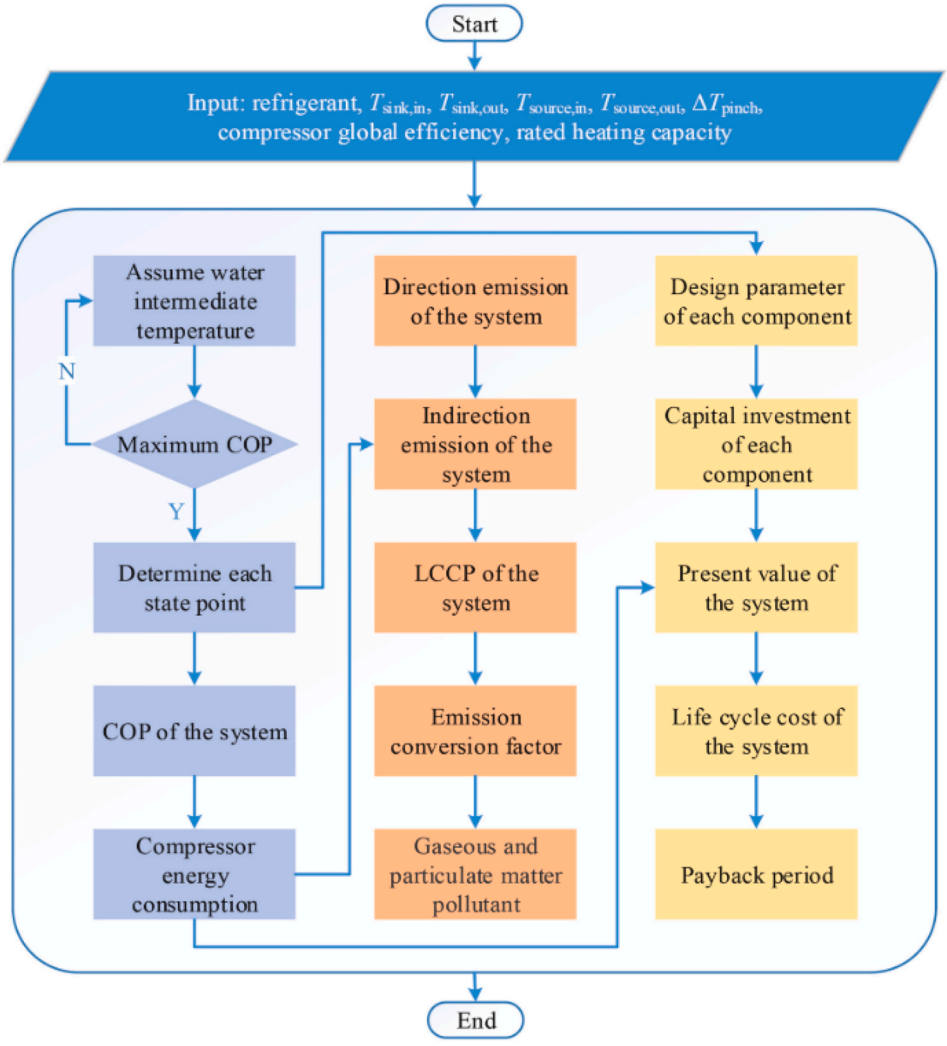

Fig. 10. HTHP economic, environmental and energetic performance analysis [119].

existing HP models are often integrated into building performance simulation programs. However, in the case of HTHPs, a more detailed approach is required, in which each of the system components is described in detail with a separate model. This also relates to the working fluid cycle analysis. This paper presents tools that can be used in model building and examples of assumptions and simplifications currently used.

Although the heat pump operates under varying conditions, most models assume steady-state conditions for the system. Therefore, it is advisable to extend the analyses to include the dynamic performance of HTHP systems, taking into account the performance of the operation during the shutdown and start-up stages. Defining the flow as homogeneous, and assuming thermodynamic equilibrium, allows strong mixing to be ensured throughout the heat exchanger operation without degrading the accuracy of the results. In addition to the challenges of HTHP modelling, the other three areas discussed are also crucial. The review shows the need to develop both high-temperature and pressure-resistant system components and environmentally friendly refrigerants that can be used in HTHP. Suitable working fluids can significantly reduce greenhouse gas emissions and contribute to a more sustainable and eco-friendly technology. Selection of appropriate components and cycle type, on the other hand, is strongly correlated with the implementation of HTHP. Therefore, further analysis of specific industries is required to match the temperature lift to the type of industrial process. Further research is therefore required to accelerate developments in this area on raising the heat sink temperature, and temperature lift while improving the COP, which would make HTHPs useful for the full range of their potential applications in the future.

Nomenclature

Abreviation	Meaning
M	Molecular weight
CFC	Chlorofluorocarbon
CFSUS	Cascade heating flash tank superheated suction system
COP	Coefficient of performance
CWSAS	Cascade-heating water cooled saturated suction system
EC	Economiser
EJ	Ejector
FT	Flash tank
GWP	Global warming potential
HC	Hydrocarbon
HCFC	Hydrochlorofluorocarbon
HCFO	Hydrocholorofluorooelfins
HFC	Hydrofluorocarbon
HFO	Hydrofluoroolefins
HP	Heat pump
HT	High temperature
HTHP	High Temperatures Heat Pump
IHX	Internal heat exchanger
LCC	Life cycle cost
MS	Multi-stage
NBP	Normal boiling point

(*continued on next page*)

(*continued*)

ODP	Ozone depletion potential
RES	Renewable energy systems
SC	Sub-cooler
SS	Single stage
VHC	Volumetric heating capacity
Symbol	Meaning
P_c	Critical pressure
Q_h	Heat released in the condenser
Q_L	Heat absorbed in the evaporator
T_c	Critical temperature

CRediT authorship contribution statement

Hussam Jouhara: Writing – review & editing, Writing – original draft, Validation, Supervision, Investigation, Funding acquisition, Conceptualization. **Alina Żabnieńska-Góra:** Writing – original draft, Methodology, Formal analysis, Data curation. **Bertrand Delpech:** Validation, Investigation. **Valentina Olabi:** Writing – original draft, Formal analysis, Data curation. **Tala El Samad:** Writing – original draft, Investigation, Formal analysis, Data curation. **Abdulnaser Sayma:** Writing – review & editing, Resources, Investigation, Conceptualization.

Declaration of competing interest

We wish to confirm that there are no known conflicts of interest associated with this publication and there has been no financial support for this work that could have influenced its outcome.

We confirm that the manuscript has been read and approved by all named authors and that there are no other persons who satisfied the criteria for authorship but are not listed. We further confirm that the order of authors listed in the manuscript has been approved by all of us.

We confirm that we have given due consideration to the protection of intellectual property associated with this work and that there are no impediments to publication, including the timing of publication, with respect to intellectual property. In so doing we confirm that we have followed the regulations of our institutions concerning intellectual property.

We understand that the Corresponding Author is the sole contact for the Editorial process (including Editorial Manager and direct communications with the office). He is responsible for communicating with the other authors about progress, submissions of revisions and final approval of proofs. We confirm that we have provided a current, correct email address which is accessible by the Corresponding Author and which has been configured to accept email from the Energy Journal.

Data availability

Data will be made available on request.

Acknowledgements

This work has received funding from the European Union's Horizon 2020 Research and Innovation Programme for projects: iWAYS, Cultural E and InComEss under Grant Agreement Numbers: 958274, 870072 and 862597 respectively.

References

[1] International Energy Agency (IEA). CO2 emissions in 2022," *CO2 emiss*. 2022. p. 2023. https://doi.org/10.1787/12ad1e1a-en.
[2] International Energy Agency (IEA). Tracking industry [Online]. Available: https://www.iea.org/energy-system/industry; 2023.
[3] European Commission. REPowerEU Affordable, secure and sustainable energy for Europe [Online]. Available: https://commission.europa.eu/strategy-and-policy/priorities-2019-2024/european-green-deal/repowereu-affordable-secure-and-sustainable-energy-europe_en; 2023.
[4] Eurostat. Final energy consumption in industry - detailed statistics [Online]. Available: https://ec.europa.eu/eurostat/statistics-explained/index.php?title=Final_energy_consumption_in_industry_-_detailed_statistics; 2023.
[5] Department for Business Energy & Industrial Strategy. Energy consumption in the UK (ECUK) 1970 to 2021. 2022.
[6] Arpagaus C, Bless F, Uhlmann M, Schiffmann J, Bertsch SS. High temperature heat pumps: market overview, state of the art, research status, refrigerants, and application potentials. Energy 2018;152:985–1010. https://doi.org/10.1016/j.energy.2018.03.166.
[7] Jouhara H. Waste heat recovery in process industries. Wiley-VCH; 2021.
[8] Bianchi G, et al. Estimating the waste heat recovery in the European Union Industry. Energy, Ecol. Environ. September, 2019. https://doi.org/10.1007/s40974-019-00132-7.
[9] Adamson KM, et al. High-temperature and transcritical heat pump cycles and advancements: a review. Renew Sustain Energy Rev 2022;167(April):112798. https://doi.org/10.1016/j.rser.2022.112798.
[10] Liu C, Jiang Y, Han W, Kang Q. A high-temperature hybrid absorption-compression heat pump for waste heat recovery. Energy Convers Manag 2018;172(July):391–401. https://doi.org/10.1016/j.enconman.2018.07.027.
[11] Austin BT, Sumathy K. Transcritical carbon dioxide heat pump systems: a review. Renew Sustain Energy Rev 2011;15(8):4013–29. https://doi.org/10.1016/j.rser.2011.07.021.
[12] Verdnik M, Rieberer R. Influence of operating parameters on the COP of an R600 high-temperature heat pump. Int J Refrig 2022;140(September 2021):103–11. https://doi.org/10.1016/j.ijrefrig.2022.05.010.
[13] Wu D, Jiang J, Hu B, Wang RZ. Experimental investigation on the performance of a very high temperature heat pump with water refrigerant. Energy 2020;190. https://doi.org/10.1016/j.energy.2019.116427.
[14] Zhang Y, et al. Analysis of a high temperature heat pump using BY-5 as refrigerant. Appl Therm Eng 2017;127:1461–8. https://doi.org/10.1016/j.applthermaleng.2017.08.072.
[15] Yu X, et al. Experimental performance of high temperature heat pump with near-azeotropic refrigerant mixture. Energy Build 2014;78:43–9. https://doi.org/10.1016/j.enbuild.2013.12.065.
[16] Chamoun M, Rulliere R, Haberschill P, Peureux J. Experimental and numerical investigations of a new high temperature heat pump for industrial heat recovery using water as refrigerant. Int J Refrig 2014;44:177–88.
[17] Wu D, Yan H, Hu B, Wang RZ. Modeling and simulation on a water vapor high temperature heat pump system. Energy 2019;168:1063–72. https://doi.org/10.1016/j.energy.2018.11.113.
[18] Sedlar J. Energy analysis of heat pump with subcooler. IEA Heat Pump Conf.; 2014. p. 1–11.
[19] Fukuda S, Kondou C, Takata N, Koyama S. Thermodynamic analysis on high temperature heat pump cycles using low-GWP refrigerants for heat recovery. In: 12th IEA heat pump conf. 2017; 2017. p. 1–7. Rotterdam.
[20] Kosmadakis G, Arpagaus C, Neofytou P, Bertsch S. Techno-economic analysis of high-temperature heat pumps with low-global warming potential refrigerants for upgrading waste heat up to 150 °C. Energy Convers Manag 2020;226(September):113488. https://doi.org/10.1016/j.enconman.2020.113488.
[21] Bai T, Yan G, Yu J. Thermodynamic assessment of a condenser outlet split ejector-based high temperature heat pump cycle using various low GWP refrigerants. Energy 2019;179:850–62. https://doi.org/10.1016/j.energy.2019.04.191.
[22] Mateu-Royo C, Navarro-Esbrí J, Mota-Babiloni A, Barragán-Cervera Á. Theoretical performance evaluation of ejector and economizer with parallel compression configurations in high temperature heat pumps. Int J Refrig 2020;119:356–65. https://doi.org/10.1016/j.ijrefrig.2020.07.016.
[23] Hao Z, Yanting Z, Jingyu X, Lin W, Zheng H. Performance analysis of internal heat exchanger-based quasi-two-stage vapor compression heat pump system for high-temperature steam production. Energy Technol 2020;8(12):1–13. https://doi.org/10.1002/ente.202000623.
[24] Kondou C, Koyama S. Thermodynamic assessment of high-temperature heat pumps using low-GWP HFO refrigerants for heat recovery. Int J Refrig 2015;53:126–41. https://doi.org/10.1016/j.ijrefrig.2014.09.018.
[25] Mateu-Royo C, Arpagaus C, Mota-Babiloni A, Navarro-Esbrí J, Bertsch SS. Advanced high temperature heat pump configurations using low GWP refrigerants for industrial waste heat recovery: a comprehensive study. Energy Convers Manag 2021;229(December 2020). https://doi.org/10.1016/j.enconman.2020.113752.
[26] Peng ZR, Wang GB, Zhang XR. Thermodynamic analysis of novel heat pump cycles for drying process with large temperature lift. Int J Energy Res 2019;43(8):3201–22. https://doi.org/10.1002/er.4394.
[27] Saikawa M, Koyama S. Thermodynamic analysis of vapor compression heat pump cycle for tap water heating and development of CO2 heat pump water heater for residential use. Appl Therm Eng 2016;106:1236–43. https://doi.org/10.1016/j.applthermaleng.2016.06.105.
[28] Fukuda S, Kondou C, Takata N, Koyama S. Low GWP refrigerants R1234ze(E) and R1234ze(Z) for high temperature heat pumps. Int J Refrig 2014;40:161–73. https://doi.org/10.1016/j.ijrefrig.2013.10.014.
[29] Ma GY, Zhao HX. Experimental study of a heat pump system with flash-tank coupled with scroll compressor. Energy Build 2008;40(5):697–701. https://doi.org/10.1016/j.enbuild.2007.05.003.
[30] Bobelin D, Bourig A, Peureux J. Experimental results of a newly developed very high temperature industrial heat pump (140°C) equipped with scroll compressors and working with a new blend refrigerant. Int. Refrig. Air Cond. Conf. 2012;2012:1–10.

[31] Hu B, Wu D, Wang LW, Wang RZ. Exergy analysis of R1234ze(Z) as high temperature heat pump working fluid with multi-stage compression. Front Energy 2017;11(4):493–502. https://doi.org/10.1007/s11708-017-0510-6.

[32] Zhang Z, Feng X, Tian D, Yang J, Chang L. Progress in ejector-expansion vapor compression refrigeration and heat pump systems. Energy Convers Manag 2020; 207(February):112529. https://doi.org/10.1016/j.enconman.2020.112529.

[33] Sarkar J. Ejector enhanced vapor compression refrigeration and heat pump systems - a review. Renew Sustain Energy Rev 2012;16(9):6647–59. https://doi.org/10.1016/j.rser.2012.08.007.

[34] Aspen Technology Inc., "Aspen Plus." [Online]. Available: https://www.aspentech.com/en/products/engineering/aspen-plus.

[35] Ma Y, Liu Z, Tian H. A review of transcritical carbon dioxide heat pump and refrigeration cycles. Energy 2013;55(2013):156–72. https://doi.org/10.1016/j.energy.2013.03.030.

[36] Lecompte S, et al. Review of experimental research on supercritical and transcritical thermodynamic cycles designed for heat recovery application. Appl Sci 2019;9(12):1–26. https://doi.org/10.3390/app9122571.

[37] Abi Chahla G, Beucher Y, Zoughaib A, de Carlan F, Pierucci J. Transcritical industrial heat pump using HFO's for up to 150°C hot air supply. Refrig. Sci. Technol. 2019;2019-Augus(1):4689–96. https://doi.org/10.18462/iir.icr.2019.1184.

[38] Kimura T, et al. Development of a high temperature heat pump using reusable heat as the heat source. In: Jraia international symposium; 2018.

[39] Verdnik M, Rieberer R. Experimental analysis of a R600 high-temperature heat pump in sub-critical and trans-critical operation. Refrig. Sci. Technol. 2020;2020 (December):500–5. https://doi.org/10.18462/iir.gl.2020.1055. Decem.

[40] Bellemo L, Gerritsen J, Hoffmann K. High temperature CO2 heat pump integration into the spray drying process. In: 2nd conference on high temperature heat pumps; 2019. p. 158–60.

[41] White SD, Yarrall MG, Cleland DJ, Hedley RA. Modelling the performance of a transcritical CO2 heat pump for high temperature heating. Int J Refrig 2002;25 (4):479–86. https://doi.org/10.1016/S0140-7007(01)00021-4.

[42] Wang JF, Brown C, Cleland DJ. Heat pump heat recovery options for food industry dryers. Int J Refrig 2018;86:48–55. https://doi.org/10.1016/j.ijrefrig.2017.11.028.

[43] Arpagaus C, Bless F, Bertsch SS. High temperature heat pumps - theoretical study on low GWP HFO and HCFO refrigerants. 25 th IIR. Int. Congr. Refrig.; August, 2019. https://doi.org/10.18462/iir.icr.2019.259.

[44] Wu D, Hu B, Wang RZ. Performance simulation and exergy analysis of a hybrid source heat pump system with low GWP refrigerants. Renew Energy 2018;116: 775–85. https://doi.org/10.1016/j.renene.2017.10.024.

[45] Li X, Wu W, Zhang X, Shi W, Wang B. Energy saving potential of low temperature hot water system based on air source absorption heat pump. Appl Therm Eng 2012;48:317–24. https://doi.org/10.1016/j.applthermaleng.2011.12.045.

[46] Kim J, et al. Experimental study of operating characteristics of compression/absorption high-temperature hybrid heat pump using waste heat. Renew Energy 2013;54:13–9. https://doi.org/10.1016/j.renene.2012.09.032.

[47] Wu W, Shi W, Wang J, Wang B, Li X. Experimental investigation on NH3-H2O compression-assisted absorption heat pump (CAHP) for low temperature heating under lower driving sources. Appl Energy 2016;176:258–71. https://doi.org/10.1016/j.apenergy.2016.04.115.

[48] Liu C, Jiang Y, Han W, Kang Q. A high-temperature hybrid absorption-compression heat pump for waste heat recovery. Energy Convers Manag 2018; 172(March):391–401. https://doi.org/10.1016/j.enconman.2018.07.027.

[49] Jensen JK, Markussen WB, Reinholdt L, Elmegaard B. Exergoeconomic optimization of an ammonia–water hybrid absorption–compression heat pump for heat supply in a spray-drying facility. Int. J. Energy Environ. Eng. 2015;6(2): 195–211. https://doi.org/10.1007/s40095-015-0166-0.

[50] Arpagaus C, Bless F, Schiffmann J, Bertsch SS. Multi-temperature heat pumps: a literature review Cordin. Int J Refrig 2016;69:437–65. https://doi.org/10.1016/j.ijrefrig.2016.05.014.

[51] Mohanraj M, Muraleedharan C, Jayaraj S. A review on recent developments in new refrigerant mixtures for vapour compression-based refrigeration, air-conditioning and heat pump units. Int J Energy Res 2011;35:647–69. https://doi.org/10.1002/er.1736.

[52] Lu Z, Yao Y, Liu G, Ma W, Gong Y. Thermodynamic and economic analysis of a high temperature. Processes 2022;10(9):1862. https://doi.org/10.3390/pr10091862.2022.

[53] Sarbu I. A review on substitution strategy of non-ecological refrigerants from vapour compression-based refrigeration, air-conditioning and heat pump systems. Int J Refrig 2014;46:123–41. https://doi.org/10.1016/j.ijrefrig.2014.04.023.

[54] Vamling L, Högberg M, Berntsson T. CFC alternatives for high-temperature heat pump applications. 1991.

[55] Göktun S. Selection of working fluids for high-temperature heat pumps. Energy 1995;20(7):623–5. https://doi.org/10.1016/0360-5442(95)00010-E.

[56] Atlanta, USA ANSI/ASHRAE standard 34, *Designation and safety Classification of refrigerants*. 2019.

[57] Fischer SK, et al. Energy and global warming impacts of CFC alternative technologies. Cambridge, MA (United States). 1991 [Online]. Available: https://www.osti.gov/biblio/5246763.

[58] Calm JM. The next generation of refrigerants - historical review, considerations, and outlook. Int J Refrig 2008;31(7):1123–33. https://doi.org/10.1016/j.ijrefrig.2008.01.013.

[59] Danfoss. "Refrigerant options now and in the future [White paper],". https://www.danfoss.com/media/7174/low-gwp-whitepaper.pdf. [Accessed 27 December 2022].

[60] McLinden MO, Brown JS, Brignoli R, Kazakov AF, Domanski PA. Limited options for low-global-warming-potential refrigerants. Nat Commun 2017;8:1–9. https://doi.org/10.1038/ncomms14476.

[61] Didion DA, Bivens DB. Role of refrigerant mixtures as alternatives to CFCs. Int J Refrig 1990;13(3):163–75. https://doi.org/10.1016/0140-7007(90)90071-4.

[62] Zühlsdorf B, Jensen JK, Cignitti S, Madsen C, Elmegaard B. Analysis of temperature glide matching of heat pumps with zeotropic working fluid mixtures for different temperature glides. Energy 2018;153:650–60. https://doi.org/10.1016/j.energy.2018.04.048.

[63] "About Montreal Protocol." [Online]. Available: https://www.unep.org/ozonaction/who-we-are/about-montreal-protocol. [Accessed 1 February 2023].

[64] Sarkar J, Bhattacharyya S, Ram Gopal M. Natural refrigerant-based subcritical and transcritical cycles for high temperature heating. Int J Refrig 2007;30(1): 3–10. https://doi.org/10.1016/j.ijrefrig.2006.03.008.

[65] Devotta S. Alternative heat pump working fluids to CFCs. Heat Recovery Syst CHP 1995;15(3):273–9. https://doi.org/10.1016/0890-4332(95)90011-X.

[66] Kazachki GS, Gage CL, Bayoglu E, Hendriks VR. Calorimeter performance tests of HFC-245ca and HFC-245fa as CFC-11 replacements. Int. Inst. Refrig.; 1993.

[67] Wu X, Tang H, Chen W, Wang X, Xing Z. Development of a high temperature heat pump for heat recovery in dyeing industry. Refrig. Sci. Technol. 2015:3777–84. https://doi.org/10.18462/iir.icr.2015.0784.

[68] He MG, Li TC, Liu ZG, Zhang Y. Testing of the mixing refrigerants HFC152a/HFC125 in domestic refrigerator. Appl Therm Eng 2005;25(8–9):1169–81. https://doi.org/10.1016/j.applthermaleng.2004.06.003.

[69] Business M. Air-sourced 90 °C hot water supplying heat pump, vol. 32; 2013. p. 70–4.

[70] Brown JS, Zilio C, Cavallini A. The fluorinated olefin R-1234ze(Z) as a high-temperature heat pumping refrigerant. Int J Refrig 2009;32(6):1412–22. https://doi.org/10.1016/j.ijrefrig.2009.03.002.

[71] Colombo LPM, Lucchini A, Molinaroli L. Experimental analysis of the use of R1234yf and R1234ze(E) as drop-in alternatives of R134a in a water-to-water heat pump. Int J Refrig 2020;115:18–27. https://doi.org/10.1016/j.ijrefrig.2020.03.004.

[72] Drofenik J, Urbancl D, Goričanec D. Comparison of the new refrigerant R1336mzz(E) with R1234ze(E) as an alternative to R134a for use in heat pumps. Processes 2022;10(2). https://doi.org/10.3390/pr10020218.

[73] Nfpa 704: standard system for the identification of the hazards of materials for emergency response [Online]. Available: https://www.nfpa.org/codes-and-standards/all-codes-and-standards/list-of-codes-and-standards/detail?code=704. [Accessed 10 January 2023].

[74] Yan H, et al. Performance prediction of HFC, HC, HFO and HCFO working fluids for high temperature water source heat pumps. Appl Therm Eng 2021;185(August 2020):116324. https://doi.org/10.1016/j.applthermaleng.2020.116324.

[75] Longo GA, Zilio C, Righetti G, Brown JS. Experimental assessment of the low GWP refrigerant HFO-1234ze(Z) for high temperature heat pumps. Exp Therm Fluid Sci 2014;57:293–300. https://doi.org/10.1016/j.expthermflusci.2014.05.004.

[76] Kondou C, Nagata R, Nii N, Koyama S, Higashi Y. Surface tension of low GWP refrigerants R1243zf, R1234ze(Z), and R1233zd(E). Int J Refrig 2015;53:80–9. https://doi.org/10.1016/j.ijrefrig.2015.01.005.

[77] Bell IH, Wronski J, Quoilin S, Lemort V. Pure and pseudo-pure fluid thermophysical property evaluation and the open-source thermophysical property library coolprop. Ind Eng Chem Res 2014;53(6):2498–508. https://doi.org/10.1021/ie4033999.

[78] Jiang J, Hu B, Wang RZ, Liu H, Zhang Z, Li H. Theoretical performance assessment of low-GWP refrigerant R1233zd(E) applied in high temperature heat pump system. Int J Refrig 2021;131:897–908. https://doi.org/10.1016/j.ijrefrig.2021.03.026.

[79] Frate GF, Ferrari L, Desideri U. Analysis of suitability ranges of high temperature heat pump working fluids. Appl Therm Eng 2019;150(January):628–40. https://doi.org/10.1016/j.applthermaleng.2019.01.034.

[80] Alhamid MI, Aisyah N, Nasruddin, Lubis A. Thermodynamic and environmental analysis of a high- temperature heat pump using HCFO-1224YD(Z) AND HCFO-1233ZD(E). Int. J. Technol. 2019;10(8):1585–92.

[81] Arpagaus C, Bless F, Uhlmann M, Büchel E, Frei S. High temperature heat pump using HFO and HCFO refrigerants - system design and experimental results. 17th Int. Refrig. Air Cond. Conf. 2018. https://doi.org/10.18462/iir.icr.2019.0242.

[82] Mateu-Royo C, Mota-Babiloni A, Navarro-Esbrí J. Semi-empirical and environmental assessment of the low GWP refrigerant HCFO-1224yd(Z) to replace HFC-245fa in high temperature heat pumps. Int J Refrig 2021;127:120–7. https://doi.org/10.1016/j.ijrefrig.2021.02.018.

[83] Mateu-Royo C, Mota-Babiloni A, Navarro-Esbrí J, Barragán-Cervera Á. Comparative analysis of HFO-1234ze(E) and R-515B as low GWP alternatives to HFC-134a in moderately high temperature heat pumps. Int J Refrig 2021;124: 197–206. https://doi.org/10.1016/j.ijrefrig.2020.12.023.

[84] Mateu-Royo C, Navarro-Esbrí J, Mota-Babiloni A, Amat-Albuixech M, Molés F. Thermodynamic analysis of low GWP alternatives to HFC-245fa in high-temperature heat pumps: HCFO-1224yd(Z), HCFO-1233zd(E) and HFO-1336mzz (Z). Appl Therm Eng 2019;152:762–77. https://doi.org/10.1016/j.applthermaleng.2019.02.047. September 2018.

[85] Mota-Babiloni A, Mateu-Royo C, Navarro-Esbrí J, Barragán-Cervera Á. Experimental comparison of HFO-1234ze(E) and R-515B to replace HFC-134a in heat pump water heaters and moderately high temperature heat pumps. Appl Therm Eng 2021;196(May). https://doi.org/10.1016/j.applthermaleng.2021.117256.

[86] Bamigbetan O, Eikevik TM, Nekså P, Bantle M, Schlemminger C. Experimental investigation of the performance of a hydrocarbon heat pump for high

temperature industrial heating. In: Refrigeration science and technology; 2018. p. 532–9. https://doi.org/10.18462/iir.gl.2018.1212. 2018-June, no. June.
[87] Bamigbetan O, Eikevik T, Nekså P, Bantle M. Evaluation of natural working fluids for the development of high temperature heat pumps. In: 2th iir gustav lorentzen natural working fluids conference; 2016. p. 575–82.
[88] Bamigbetan O, Eikevik TM, Nekså P, Bantle M. Review of vapour compression heat pumps for high temperature heating using natural working fluids. Int J Refrig 2017;80:197–211. https://doi.org/10.1016/j.ijrefrig.2017.04.021.
[89] Stavset O, Banasiak K, Hafner A. Analysis of high temperature heat pumps applying natural working fluids. In: Proceedings of the 11th IIR-gustav lorentzen conference on natural refrigerants GL2014; 2014.
[90] Bamigbetan O, Eikevik TM, Nekså P, Bantle M, Schlemminger C. The development of a hydrocarbon high temperature heat pump for waste heat recovery. Energy 2019;173:1141–53. https://doi.org/10.1016/j.energy.2019.02.159.
[91] Pohanish RP. Toxic and hazardous chemicals and carcinogens [Online]. Available: http://www.sciencedirect.com:5070/book/9780323389686/sittigs-handbook-of-toxic-and-hazardous-chemicals-and-carcinogens; 2017. 03-Jan-2023.
[92] Zhang J, Zhang HH, He YL, Tao WQ. A comprehensive review on advances and applications of industrial heat pumps based on the practices in China. Appl Energy 2016;178:800–25. https://doi.org/10.1016/j.apenergy.2016.06.049.
[93] Huang T, Yuan DL. Application of heat pump water heating system with heat recovery in ammonia refrigeration system. Adv Mater Res 2012;614(615):670–3. https://doi.org/10.4028/www.scientific.net/AMR.614-615.670.
[94] Chamoun M, Rulliere R, Haberschill P, Peureux JL. Experimental and numerical investigations of a new high temperature heat pump for industrial heat recovery using water as refrigerant. Int J Refrig 2014;44:177–88. https://doi.org/10.1016/j.ijrefrig.2014.04.019.
[95] Madsboell H, Weel M, Kolstrup A. Development of a water vapor compressor for high temperature heat pump applications. In: Refrigeration science and technology; 2015. p. 1613–20. https://doi.org/10.18462/iir.icr.2015.0845.
[96] Nekså P, Rekstad H, Zakeri GR, Schiefloe PA. CO2-heat pump water heater: characteristics, system design and experimental results. Int J Refrig 1998;21(3):172–9. https://doi.org/10.1016/S0140-7007(98)00017-6.
[97] Dai B, et al. Life cycle techno-enviro-economic assessment of dual-temperature evaporation transcritical CO2 high-temperature heat pump systems for industrial waste heat recovery. Appl Therm Eng 2023;219(PB):119570. https://doi.org/10.1016/j.applthermaleng.2022.119570.
[98] Weck-Ponten S, Frisch J, van Treeck C. Simplified heat pump system model integrated in a tool chain for digitally and simulation-based planning shallow geothermal systems. Geothermics 2022;106(June):102579. https://doi.org/10.1016/j.geothermics.2022.102579.
[99] Zirngibl J. Heat pump standard EN 15316-4-2 – from compliance to real consumption. REHVA J 2020;6(December):5–9.
[100] TRNSYS transient system simulation tool [Online]. Available: http://www.trnsys.com/. [Accessed 15 September 2023].
[101] Zanetti E, Bordignon S, Conte R, Bisi A, Azzolin M, Zarrella A. Experimental and numerical analysis of a CO2 dual-source heat pump with PVT evaporators for residential heating applications. Appl Therm Eng 2023;233(July). https://doi.org/10.1016/j.applthermaleng.2023.121165.
[102] Bordignon S, Emmi G, Zarrella A, De Carli M. Energy analysis of different configurations for a reversible ground source heat pump using a new flexible TRNSYS Type. Appl Therm Eng 2021;197(April):117413. https://doi.org/10.1016/j.applthermaleng.2021.117413.
[103] National Institute of Standards and Technology (NIST), "NIST Reference Fluid Thermodynamic and Transport Properties Database (REFPROP): Version 10." [Online]. Available: https://www.nist.gov/srd/refprop. [Accessed: 15-Sep-2023].
[104] Lu Z, Ziviani D. Operating cost comparison of state-of-the-art heat pumps in residential buildings across the United States. Energy Build 2022;277:112553. https://doi.org/10.1016/j.enbuild.2022.112553.
[105] U.S. Department of energy's, "EnergyPlus,". 2023 [Online]. Available: https://energyplus.net/quick-start#what. [Accessed 15 September 2023].
[106] Shen B, New J, Baxter V. Air source integrated heat pump simulation model for EnergyPlus. Energy Build 2017;156:197–206. https://doi.org/10.1016/j.enbuild.2017.09.064.
[107] Hassan AH, Corberán JM, Ramirez M, Trebilcock-Kelly F, Payá J. A high-temperature heat pump for compressed heat energy storage applications: design, modeling, and performance. Energy Rep 2022;8:10833–48. https://doi.org/10.1016/j.egyr.2022.08.201.
[108] Bamigbetan O, Eikevik TM, Nekså P, Bantle M, Schlemminger C. Theoretical analysis of suitable fluids for high temperature heat pumps up to 125 °C heat delivery. Int J Refrig 2018;92:185–95. https://doi.org/10.1016/j.ijrefrig.2018.05.017.
[109] Mateu Royo C, Navarro-Esbrí J, Mota-Babiloni A, Amat-lbuixech M, Molés F. Development of high temperature heat pumps for industrial waste heat recovery. Universitat Jaume; 2021 [Online]. Available: https://search.ebscohost.com/login.aspx?direct=true&db=edstdx&AN=edstdx.10803.672558&amp%0Alang=pt-pt&site=eds-live&scope=site.
[110] Mota-Babiloni A, Mateu-Royo C, Navarro-Esbrí J, Molés F, Amat-Albuixech M, Barragán-Cervera Á. Optimisation of high-temperature heat pump cascades with internal heat exchangers using refrigerants with low global warming potential. Energy 2018;165:1248–58. https://doi.org/10.1016/j.energy.2018.09.188.
[111] National Institute of Standards and Technology (NIST), "NIST Reference Fluid Thermodynamic and Transport Properties Database (REFPROP): Version 10." [Online]. Available: https://www.nist.gov/srd/refprop. [Accessed: 15-Sep-2023].
[112] Huber ML, Lemmon EW, Bell IH, McLinden MO. The NIST REFPROP database for highly accurate properties of industrially important fluids. Ind Eng Chem Res 2022;61(42):15449–72. https://doi.org/10.1021/acs.iecr.2c01427.
[113] "F-Chart Software," *Engineering Equation Solver*. [Online]. Available: https://fchartsoftware.com/ees/. [Accessed: 02-Mar-2023].
[114] Hong T, Sun K, Zhang R, Hinokuma R, Kasahara S, Yura Y. Development and validation of a new variable refrigerant flow system model in EnergyPlus. Energy Build 2016;117:399–411. https://doi.org/10.1016/j.enbuild.2015.09.023.
[115] Arpagaus C, Prinzing M. High temperature heat pumps - theoretical study on low GWP HFO and HCFO refrigerants. In: 25th IIR international congress of refrigeration. Refrigeration science and technology proceedings; 2019. https://doi.org/10.18462/iir.icr.2019.259. August.
[116] Liu Y, Groll EA, Yazawa K, Kurtulus O. Économies d'énergie et financières enregistrées sur les pompes à chaleur fonctionnant au CO2 et au NH3 dans des applications de chauffage et de refroidissement simultanés pour l'industrie agroalimentaire : études de cas. Int J Refrig 2017;73:111–24. https://doi.org/10.1016/j.ijrefrig.2016.09.014.
[117] Liu Y, Groll EA, Yazawa K, Kurtulus O. Theoretical analysis of energy-saving performance and economics of CO2 and NH3 heat pumps with simultaneous cooling and heating applications in food processing. Int J Refrig 2016;65:129–41. https://doi.org/10.1016/j.ijrefrig.2016.01.020.
[118] Zhao Z, Gao S, Tian Y, Zhang H. Study on performance of high temperature heat pump system integrated with flash tank for waste heat recovery employed in steam production. Int J Energy Res 2021;45(14):20318–30. https://doi.org/10.1002/er.7116.
[119] Dai B, et al. Life cycle performance evaluation of cascade-heating high temperature heat pump system for waste heat utilization: energy consumption, emissions and financial analyses. Energy 2022;261(PB):125314. https://doi.org/10.1016/j.energy.2022.125314.
[120] Obrist MD, Kannan R, McKenna R, Schmidt TJ, Kober T. High-temperature heat pumps in climate pathways for selected industry sectors in Switzerland. Energy Pol 2023;173(November 2022):113383. https://doi.org/10.1016/j.enpol.2022.113383.
[121] Schlosser F, Zysk S, Walmsley TG, Kong L, Zühlsdorf B, Meschede H. Break-even of high-temperature heat pump integration for milk spray drying. Energy Convers Manag 2023;291(June):117304. https://doi.org/10.1016/j.enconman.2023.117304.
[122] Walden JVM, Bähr M, Glade A, Gollasch J, Tran AP, Lorenz T. Nonlinear operational optimization of an industrial power-to-heat system with a high temperature heat pump, a thermal energy storage and wind energy. Appl Energy 2023;344(March 2022):121247. https://doi.org/10.1016/j.apenergy.2023.121247.
[123] Nowak T. Heat Pumps: integrating technologies to decarbonise heating and cooling. Eur. Copp. Inst.; 2018. p. 1–86.
[124] International Energy Agency (IEA). Renewables 2023. 2023.
[125] International Energy Agency (IEA). The future of heat pumps. 2022.
[126] Gaur AS, Fitiwi DZ, Curtis J. Heat pumps and our low-carbon future: a comprehensive review. Energy Res Social Sci 2021;71:101764. https://doi.org/10.1016/j.erss.2020.101764. August 2020.
[127] Tveit T-M, Khan U, Zevenhoven R. Environmental impact of high temperature industrial heat pumps from a global warming potential (GWP) perspective. Ind. Effic. 2020:14–6.
[128] Li X, et al. Energy, exergy, economic, and environmental analysis of an integrated system of high-temperature heat pump and gas separation unit. Energy Convers Manag 2019;198(May):111911. https://doi.org/10.1016/j.enconman.2019.111911.
[129] Urbanucci L, Bruno JC, Testi D. Thermodynamic and economic analysis of the integration of high-temperature heat pumps in trigeneration systems. Appl Energy 2019;238(January):516–33. https://doi.org/10.1016/j.apenergy.2019.01.115.